Universidade de Aveiro Departamento de Química
2017

Antoine Simões Almeida

Avaliação do potencial inflamatório de aerossóis orgânicos inaláveis presentes em uma atmosfera urbana

Assesment of the inflammatory potential of inhalable organic aerosols present in an urban atmosphere

Universidade de Aveiro Departamento de Química
2017

Antoine Simões Almeida

Avaliação do potencial inflamatório de aerossóis orgânicos inaláveis presentes em uma atmosfera urbana

Assesment of the inflammatory potential of inhalable organic aerosols present in an urban atmosphere

Dissertação apresentada à Universidade de Aveiro para cumprimento dos requisitos necessários à obtenção do grau de Mestre em Bioquímica, ramo de Bioquímica Clínica, realizado sob a orientação científica da Doutora Regina Maria Brandão de Oliveira Duarte, equiparada a Investigadora Principal do Centro de Estudos do Ambiente e do Mar (CESAM) da Universidade de Aveiro, e do Doutor Bruno Miguel Rodrigues das Neves, Professor Auxiliar convidado da Faculdade de Farmácia da Universidade de Coimbra

o júri

presidente

Prof. Doutora Maria do Rosário Gonçalves dos Reis Marques Domingues
Professora Associada com Agregação do Departamento de Química da Universidade de Aveiro

Doutora Regina Maria Brandão de Oliveira Duarte
Equiparada a Investigador Principal do Centro de Estudos do Ambiente e do Mar da Universidade de Aveiro

Prof. Doutora Rita Maria Pinho Ferreira
Professora Auxiliar do Departamento de Química da Universidade de Aveiro

agradecimentos

Aos meus orientadores, Doutora Regina Duarte e Professor Doutor Bruno Neves, pelo apoio, dedicação, contribuição e pela disponibilidade demonstrada durante a realização deste trabalho.

Ao Professor Doutor Artur Silva, pela disponibilidade para a aquisição dos espetros de RMN uni- e bidimensionais e pela sua contribuição e ajuda na interpretação destes mesmos espetros.

À Professora Doutora Rita Ferreira, pela disponibilidade e colaboração na realização dos ensaios de atividade antioxidante *in chemico*.

Ao Professor Doutor Armando Duarte, pela disponibilidade de meios, recursos laboratoriais e financeiros que muito contribuíram para os resultados alcançados neste trabalho, bem como para a respetiva divulgação.

Aos colegas de laboratório, em especial ao Doutor João Matos, pela sua disponibilidade e ajuda prestadas na realização deste trabalho, nomeadamente na aquisição dos espetros de fluorescência e na análise de carbono orgânico dissolvido nos extratos aquosos das amostras de partículas atmosféricas

Ao Centro de Estudos do Ambiente e do Mar (CESAM) da Universidade de Aveiro pelo suporte financeiro, nomeadamente na aquisição de material e reagentes utilizados na realização deste trabalho.

À minha família e amigos pelo seu incansável apoio e suporte.

palavras-chave

Aerossóis atmosféricos; Matéria particulada fina; Carbono orgânico solúvel em água; Partículas inaláveis; Imunidade inata; Inflamação; Stress oxidativo

resumo

A matéria particulada (sigla inglesa, *PM*) é definida como uma suspensão de partículas sólidas ou líquidas num gás (*i.e.*, atmosfera), sendo estas tipicamente classificadas de acordo com o seu tamanho: PM_{10} (diâmetro aerodinâmico < 10μm), $PM_{2.5}$ (diâmetro aerodinâmico < 2.5μm) e $PM_{1.0}$ (diâmetro aerodinâmico <1.0μm). Estas partículas podem ser emitidas diretamente para a atmosfera através de fontes antropogénicas ou naturais, ou formadas *in situ* na atmosfera através de processos físico-químicos. A *PM* tem impacto relevante não só em processos atmosféricos e climáticos, mas também na saúde humana, onde se destaca o aumento de risco de doenças pulmonares e cardiovasculares, o aumento de suscetibilidade a infeções, e efeitos carcinogénicos e mutagénicos. Particularmente, ao nível pulmonar, os principais efeitos da *PM* descritos na literatura incluem a indução de stress oxidativo e da inflamação, podendo levar a danos pulmonares. O conhecimento dos efeitos nocivos das *PM* para a saúde pública resulta fundamentalmente de estudos realizados com as partículas, sendo a contribuição da fração de matéria orgânica solúvel em água (sigla inglesa, *WSOM*) pouco abordada. Neste sentido, o presente trabalho procura caracterizar a fração *WSOM* de $PM_{2.5}$, recolhida durante o período de outono, e avaliar os seus efeitos em macrófagos. A caracterização estrutural, com recurso à técnica de espectroscopia de ressonância magnética nuclear de protão (RMN ^{1}H), mostra que as amostras *WSOM* recolhidas no período noturno apresentam um maior conteúdo de estruturas aromáticas e oxigenadas do que as amostras recolhidas no período diurno, com estas últimas a apresentarem maior conteúdo em estruturas alifáticas. Adicionalmente, a caracterização das amostras *WSOM* com recurso à espectroscopia de RMN bidimensional (2D) permitiu identificar diferentes componentes estruturais e determinar possíveis fontes destas estruturas. Os ensaios biológicos de exposição aguda (24h) de macrófagos às amostras *WSOM* demonstraram que tanto as amostras diurnas como noturnas induzem um aumento da transcrição da enzima destoxificante *Hmox*, como das moléculas pro-inflamatórias *Il1b*, *Il6* e *Nos2*. Observou-se também que os extratos apresentam atividade antioxidante *in chemico* e *in vitro*. Em ensaios de exposição prolongada (3 semanas) a concentrações fisiologicamente relevantes observou-se um pequeno aumento na transcrição dos genes estudados. No entanto, verificou-se que estes macrófagos apresentavam uma capacidade limitada de resposta a um agente inflamatório como o Lipopolissacarídeo bacteriano (LPS).

De uma forma geral, os resultados obtidos indicam que a exposição prolongada a *WSOM* presente nas partículas atmosféricas pode provocar um ligeiro estado inflamatório a nível pulmonar, limitando, no entanto, a capacidade de resposta dos macrófagos a agentes invasores, o que pode originar um aumento da suscetibilidade a infeções.

keywords

Atmospheric aerosols; Fine particulate matter; Water-soluble organic carbon; Inhalable particles; Innate immunity; Inflammation; Oxidative stress.

abstract

Airborne particulate matter (PM), are defined as solid or liquid particles suspended in a gas (*i.e.*, atmosphere), and are typically distributed in three size-ranges: PM_{10} (coarse PM, aerodynamic diameter < 10μm), $PM_{2.5}$ (fine PM, aerodynamic diameter < 2.5μm) and $PM_{1.0}$ (ultrafine PM, aerodynamic diameter < 1.0μm). These particles can be emitted directly into the atmosphere from both anthropogenic and natural sources, or formed *in situ* in the atmosphere through physico-chemical processes. The PM plays a significant role in diverse atmospheric and climatic processes, as well as on human health by increasing the risk of cardiovascular and pulmonary diseases, the susceptibility to infections, and having carcinogenic and mutagenic effects. Particularly, in the lungs, the main effects of PM described in the literature include the induction of oxidative stress and inflammation, occasionally leading to lung injury. The knowledge of the harmful effects of PM on public health is fundamentally due to studies carried out with particles, being the contribution of the fraction of water-soluble organic matter (WSOM) largely unknown. Therefore, the present work aims to characterize the WSOM fraction of $PM_{2.5}$, collected during autumn season, and assess its effects on macrophages. The structural characterization of the WSOM from atmospheric particles, by means of proton nuclear magnetic resonance (^{1}H NMR) spectroscopy, showed that samples collected during the night have higher content of aromatic and oxygenated structures than those collected during the day, with the later exhibiting higher content of aliphatic structures. Furthermore, the structural characterization of the WSOM samples by means of two-dimensional (2D) NMR spectroscopy also allowed the identification of different structural components and the tentative assignment of their sources. The biological assays on the effect of an acute exposure (24h) to the WSOM samples showed that both day and night samples induced an increase in the transcription of the detoxifying enzyme *Hmox*, and the pro-inflammatory molecules *Il1b*, *Il6* and *Nos2*. It was also observed that these extracts present antioxidant activity *in chemico* and *in vitro*. In the biological assays of prolonged exposure (3 weeks) at physiologically relevant concentrations, it was observed a small increase in the transcription of the studied genes. However, the obtained data show that these macrophages present a limited capacity to respond to an inflammatory agent such as bacterial lipopolysaccharide (LPS).

In general, the obtained results show that a prolonged exposure to WSOM present in atmospheric particles can induce or worsen an inflammatory response at the pulmonary level, leading however, to a limited capacity of response of the macrophages to invading agents which could increase the susceptibility to infections.

Table of Contents

List of figures

List of tables

List of abbreviations

COX	Cyclooxygenase
DEP	Diesel exhaust particles
DNA	Deoxyribonucleic acid
EC	Elemental carbon
EDX	Energy dispersive X-ray
IL	Interleukin
MAPK	Mitogen-activated protein kinases
NF-kB	Nuclear factor-kB
NOS	Nitric oxide synthase
OC	Organic carbon
PAF	Platelet-activating factor
PAHs	Polycyclic aromatic hydrocarbons
PM	Particulate matter
$PM_{1.0}$	Particulate matter with aerodynamic diameter less than 1.0 μm
$PM_{2.5}$	Particulate matter with aerodynamic diameter less than 2.5μm
PM_{10}	Particulate matter with aerodynamic diameter less than 10 μm
RNS	Reactive nitrogen species
ROS	Reactive oxygen species
SEM	Scanning electron microscopy
SOA	Secondary organic aerosols
SOD	Super oxide dismutase
TGF-β	Transforming growth factor-β
TNF	Tumor necrosis factor
VOCs	Volatile organic compounds
WSOC	Water soluble organic carbon
WSOM	Water soluble organic matter

Chapter 1

Introduction

1.1. Atmospheric particles: sizes, composition, and their effect on human health

1.1.1 An overview of the classification and chemical composition of atmospheric particles

Atmospheric aerosols, also referred in the literature as airborne particulate matter (PM), are defined as solid or liquid particles suspended in a gas (*i.e.*, atmosphere), whose diameters range from over 100μm to about 1nm (Seinfeld and Pandis, 2006). In relation to their size, the PM are usually distributed among three size ranges: PM_{10}, $PM_{2.5}$ and $PM_{1.0}$. The PM_{10} is also called as "coarse PM", and it includes air particles whose aerodynamic diameter measure less than 10μm. The $PM_{2.5}$ is usually named "fine PM", and it comprises air particles whose aerodynamic diameters is less than 2.5μm, and finally the $PM_{1.0}$ is considered as "ultrafine PM" with an aerodynamic diameter less than 1.0μm. Due to their small sizes, the atmospheric particles with diameters less than 2.5μm can pass through the human body's physical barriers, being therefore inhalable and thus reach the lungs (Miller et al., 1979). This makes the study of the interactions between these particles and the organism particularly relevant.

As schematically illustrated in Figure 1, atmospheric particles can be emitted directly into the atmosphere as a result of anthropogenic activities, such as traffic emissions (*i.e.* exhaust emissions, brakes and tire deterioration), wood burning in domestic fireplaces, industrial processes, and resuspension of soil dust caused by road traffic. Atmospheric aerosols can also be emitted from natural sources, such as volcano eruptions, sea spray from wave bursting, soil particles resuspension due to wind erosion, as well as from the biosphere (*e.g.* pollen release, and volatile organic compounds (VOCs) emissions from trees and plants) (Gelencsér et al., 2007; Schauer et al., 1996). These particles released directly into the atmosphere are typically classified as primary aerosols. In turn, secondary aerosols comprise the particles formed in the atmosphere through gas-to-particle conversion processes, including the oxidation of precursor gases, such as sulphur dioxide, nitrogen oxides, and biogenic and anthropogenic VOCs. Once in the atmosphere, the primary atmospheric particles can also undergo chemical and physical transformations, by condensation of vapor species, evaporation, coagulation with other particles, and chemical reactions (Atkinson, 2000).

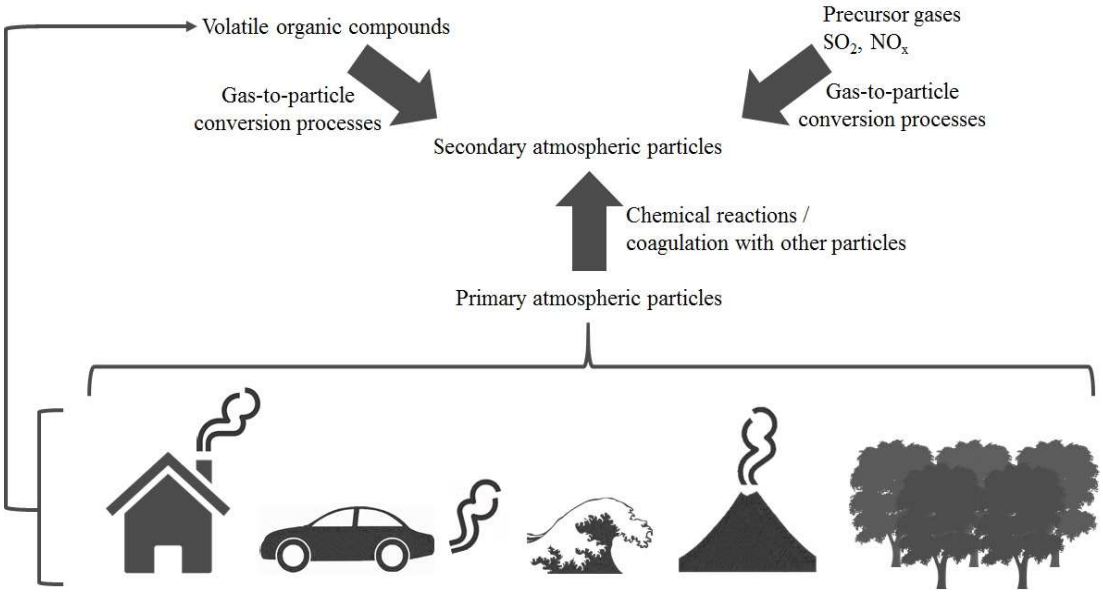

Figure 1. Schematic representation of primary and secondary sources of atmospheric particles.

In terms of chemical composition, PM is generally composed of variable amounts of carbonaceous material, consisting of elemental carbon (EC) and organic carbon (OC), as well as trace metals (*e.g.* Cu, Zn, Sr, Ni, Cd, Pb), crustal elements (*e.g.* Al, Si, Mg, Mn, Fe, Ca) and inorganic ions such as sulphate (SO_4^{2-}), nitrate (NO_3^-), ammonium (NH_4^+), carbonate (CO_3^{2-}), sodium (Na^+), and chloride (Cl^-) (Calvo et al., 2013) (Figure 2). The EC has a primary origin and it is mainly derived from fossil-related sources, whereas the main sources of the OC component differ between seasons (*i.e.*, summer and winter). In warmer conditions, the main contributor to the OC are secondary organic aerosols (SOA) originated from precursors emitted from non-fossil sources, with some minor contribution from fossil fuel combustion sources. In cold seasons, the main source of OC are primary emissions from biomass burning, alongside some contribution from fossil fuel combustion sources. Both OC and EC are preferentially present in fine-size particles (Gelencsér et al., 2007). As for the sources of trace metals, which are also preferentially found in fine-size PM, they arise from anthropogenic activities including traffic, residual oil combustion, and industrial processes. The crustal material (*e.g.* CO_3^{2-}, Si, Al, Fe, Ca, and Mn) and sea spray (*e.g.* Mg, Na, and Cl), are usually found in the coarse PM fraction. Wind erosion, primary emissions, mechanical disruption, sea spray, and volcanic eruptions, they all contribute to the atmospheric concentrations of these species (Gelencsér et al., 2007; Seinfeld and Pandis, 2006; Senesi et

al., 2009). The inorganic ions SO_4^{2-}, NO_3^-, and NH_4^+ are present mainly in the fine-size mode, and typically have a secondary origin (Senesi et al., 2009).

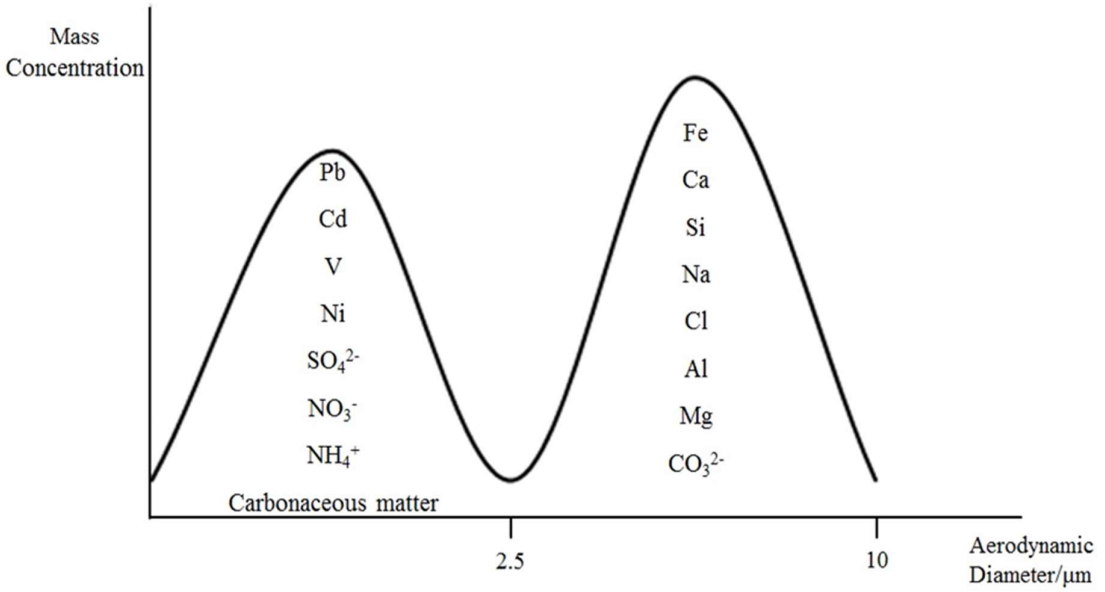

Figure 2. A typical aerosol mass size distribution profile showing a typical segmentation of chemical species into fine (aerodynamic diameter < 2.5μm) and coarse (2.5 < aerodynamic diameter < 10 μm) modes (adapted from (Samara and Voutsa, 2005; Seinfeld and Pandis, 2006)).

Once in the atmosphere, the PM will undergo some specific processes that lead to their removal from the atmosphere. For the PM close to the ground (altitudes under 100m), the main deposition mechanism is dry deposition (*e.g.* settling and impaction on surfaces), whereas the PM present at higher altitudes are predominantly removed by wet deposition processes (i.e. deposition caused by precipitation processes, such as rain or snow) (Seinfeld and Pandis, 2006). The residence time of PM in the atmosphere depends on its size: the deposition of coarse PM occurs within some hours after their emission due to their large size, leading to their deposition close to the emission sources. On the other hand, fine PM have residences times in the order of days (from a few days to a week) due to their small sizes, which leads to their deposition on locations far away from their emission sources (Seinfeld and Pandis, 2006). The residence time of PM has important implications on their own physico-chemical characteristics, since during their atmospheric transportation, the PM can undergo chemical transformations, such as photo-oxidation (secondary aerosols formation) that alters the chemical properties of the particles (Seinfeld and Pandis, 2006).

The PM can also have various shapes, as shown in Figure 3. This figure shows photos obtained from scanning electron microscopy (SEM) analysis of different atmospheric particles: Figure 3a exhibits a SEM image of a section of a Teflon filter with atmospheric PM deposited onto its surface; Figures 3b and 3c show the SEM images of two different atmospheric particles and their main elemental composition obtained by means of energy dispersive X-ray (EDX) spectroscopy - in particular, Figure 3c clearly shows the cubic shape of a sodium chloride crystal.

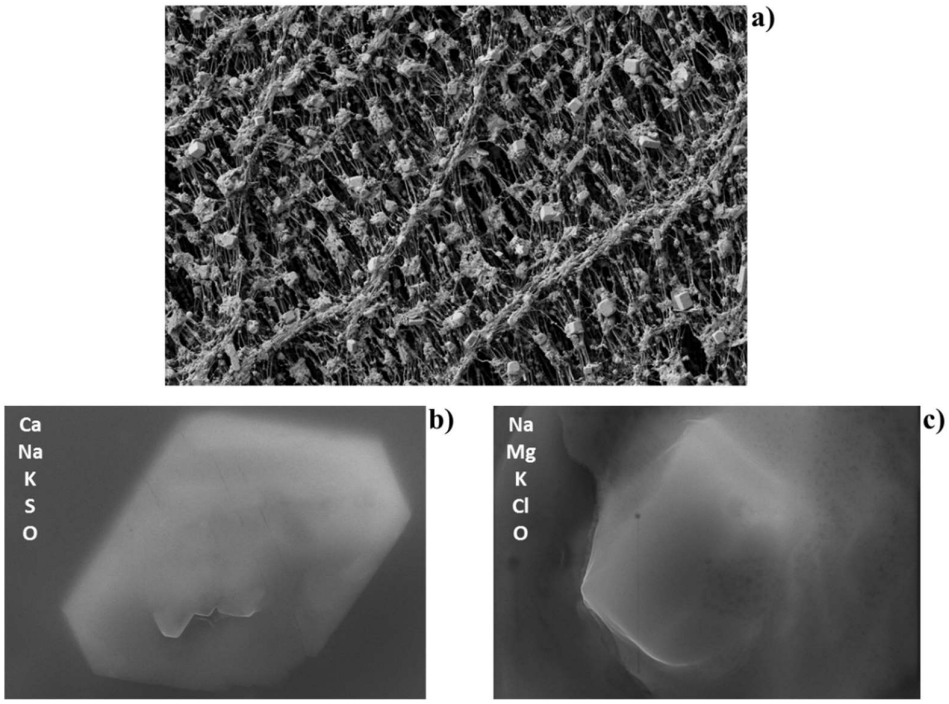

Figure 3. SEM images of different atmospheric particles with aerodynamic diameter less than 2.5μm (photos by courtesy of ORGANOSOL research project, PTDC/CTE-ATM/118551/2010, https://organosolproject.wordpress.com/).

1.1.2 Chemical composition of inhalable fine particulate matter

As previously described, $PM_{2.5}$ are composed roughly of a carbonaceous fraction, trace metals, crustal elements, and inorganic ions. The contribution of each of these components to the total mass of the particle depends on a set of factors, such as the distance from the emission source as well as the emission source itself (Calvo et al., 2013; Putaud et al., 2010). Figure 4 shows a schematic representation of the average composition of $PM_{2.5}$ samples in Europe.

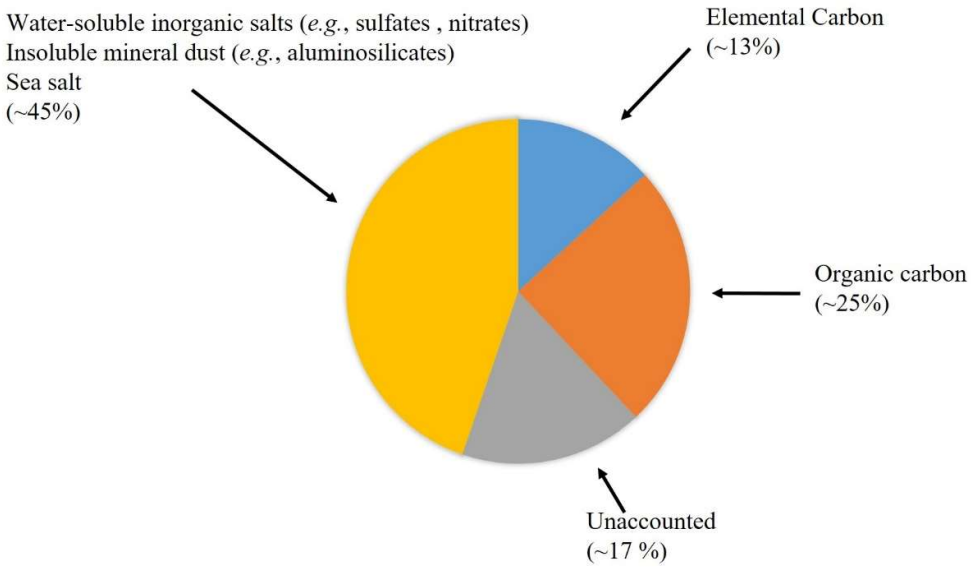

Figure 4. Schematic representation of the chemical composition of $PM_{2.5}$ in Europe (adapted from (Putaud et al., 2010)).

In $PM_{2.5}$, the EC accounts on average to 13% of the mass of the air particles, ranging from 6% to 25%. The lowest EC contents are usually found in remote areas, such as mountain tops and rural areas, whereas the highest EC values are typically reported for urban and industrial areas, with percentage values as high as 25% of the aerosol mass being measured in road tunnels (Putaud et al., 2010). As for the OC component, the average mass percentage of this organic fraction is about 25%, ranging between 20% and 30%, but it can reach percentage values up to 36% in locations with lower EC emissions. The OC component is further comprised of a water-insoluble organic carbon and water-soluble organic carbon (WSOC) fractions, with the latter accounting for 10 to 80% of the OC fraction (Duarte et al.,

2016; Duarte and Duarte, 2011). As recently reviewed by Duarte and co-workers (Duarte et al., 2016), the WSOC fraction is particularly important due to its important role in several atmospheric processes. The WSOC might potentially affect the properties that determine the PM ability to act as cloud condensation nuclei (Dinar et al., 2006; Padró et al., 2010). It has been also suggested that the WSOC might contribute to the absorption of solar radiation, and thus atmospheric heating and global climate change (Dinar et al., 2008; Mladenov et al., 2010). Furthermore, the wet deposition fluxes of atmospheric WSOC indicate that it may be an important temporal source of OC to surface waters and, thus, playing an important role in the global carbon cycle (Jurado et al., 2008). From the public health perspective, there are evidences on the association between aerosol OC and adverse health effects (Cassee et al., 2013), with the secondary OC component (more water-soluble) being suggested as a valuable air quality metric. Lower percentages of WSOC are usually found in urban areas, whereas higher WSOC contents are found in remote locations, such as mountain tops and rural areas (Anderson et al., 2008). This geographic distribution can be explained by the distance from the emission sources, with the $PM_{2.5}$ samples collected in more remote locations having a higher WSOC content due to the longer distances travelled by these particles as compared to those collected at urban centers, thus allowing them to suffer chemical transformations (secondary aerosols formation), leading to an increase in the WSOC content (Duarte et al., 2016; Duarte and Duarte, 2011). The water-soluble inorganic salts (such as NO_3^- and SO_4^{2-}) account for about 40% (26% to 46%) of the $PM_{2.5}$ mass, while the insoluble mineral dust accounts for about 4% of the $PM_{2.5}$ mass, and the sea salt only accounts for about 1% of the mass particle (1% to 2%) (Putaud et al., 2010). The water-soluble inorganic salts are mainly formed through secondary processes in the atmosphere and, therefore, it is expected to observe a higher content of these compounds in rural environments due to a higher travel distance from the emission sources being subjected to more secondary processes in the atmosphere (Putaud et al., 2010). The atmospheric content of these compounds follow also a seasonal trend, with the SO_4^{2-} being found in higher concentrations during warm seasons, whereas NO_3^- are found in higher concentrations during cold seasons (Seinfeld and Pandis, 2006).

1.1.3 Effects of atmospheric particulate matter on human health

The effects of atmospheric particles on human health have been studied throughout several epidemiological and experimental studies. These studies evidenced the noxious

effects of the exposure to high levels of PM, namely the increased risks of respiratory and cardiovascular diseases and lung cancer (Hoek et al., 2013; Kim et al., 2015; Pope et al., 2002). For instance, Pope and co-workers (Pope et al., 2002) studied the effects of long term exposure to fine particulate air pollution on lung cancer and cardiopulmonary related mortality. The authors concluded that an increase of 10μg m^{-3} in atmospheric concentration of $PM_{2.5}$ was associated with an increase of 6% and 8% in cardiopulmonary and lung cancer mortality risk, respectively. On the other hand, in another study, the same group of authors also reported that a decrease in 10μg m^{-3} of the concentration of $PM_{2.5}$ was associated with an increase in live expectancy of about 0.61±0.20 years (Pope et al., 2009).

Reviewing the toxicity and health impact of different PM constituents, Schwarze *et al* (Schwarze et al., 2006) concluded that metals appear to have an important role in the development of cardiovascular and pulmonary diseases. Additionally, and in spite the short experimental evidence of the effects of the crustal elements, epidemiological studies have shown that these particles may have adverse effects on respiratory morbidity. There has been also reported a high human health risk associated with the mutagenic and carcinogenic effects of the exposure to polycyclic aromatic hydrocarbons (PAHs) present in anthropogenic-related air particles (Mazzeo, 2011), as well as the oxidative stress-induced damage on deoxyribonucleic acid (DNA) caused by the exposure to diesel exhaust particles (DEP) (Risom et al., 2005). Finally, exposure to PM also affects the immune system, increasing the susceptibility to infections and pathogens, or aggravating preexisting lung diseases such as asthma (Bauer et al., 2012; Jang, 2012).

Overall, current data demonstrate the negative impact to PM exposure in terms of human health, and emphasize the importance of implementing mitigation strategies to diminish and limit the emission of fine particles into the atmosphere. In this regard, the European Union created the 2008/50/EC directive, which set the limit levels for the emission of PM in its member states. For the $PM_{2.5}$ emissions, the European annual threshold by the year of 2015 was set at 20μg m^{-3}, based upon measurements in urban background locations.

1.2. The innate immune response to inhaled atmospheric particles

The toxicity of inhaled atmospheric particles and their deleterious effects in human health is in great part due to the induction or exacerbation of a preexisting inflammatory condition. It is therefore important to briefly overview the inflammatory process and their innate immune effectors in order to understand how air particles affect body homeostasis.

1.2.1 Inflammation: a look on the body defense mechanisms

Inflammation is the organism primary mechanism of defense against infections (fungal, bacterial, parasitic or viral), damaged/necrotic cells, and foreign bodies (dirt, splinters or sutures). Even though it is a protective response with the aim of reestablish homeostasis, if exacerbated or sustained in time, inflammation has serious harmful effects to the host. This process can be sorted as acute or chronic depending on the cells involved in its development and resolution. The former is characterized by a short duration, ranging from minutes to a few days, by neutrophilic leukocyte accumulation, fluid and plasma proteins exudation and by a mild level of tissue injury with limited fibrosis. On the other hand, chronic inflammation is characterized by a longer duration, from days to years, by vascular proliferation, influx of lymphocytes and macrophages and severe tissue damage with progressive fibrosis. Additionally, in acute inflammation the systemic and local signs are prominent, whereas in chronic inflammation they are more subtle (Kumar et al., 2010; Serhan, 2010). The inflammatory process is orchestrated by innate immune cells such as neutrophils, macrophages, and dendritic cells and comprises a series of physiological alterations that manifest into the five cardinal signs of inflammation: pain, redness, swelling, heat, and loss of function. The first four signs were known for a long time being described by Celsus, a roman writer of the 1st century AD, whereas the latter (loss of function), was described by Rudolf Virchow in the 19th century (Kumar et al., 2010).

As illustrated in Figure 5, the kinetics of the inflammatory process can be resumed in four main events: phase 1: the vasodilation resulting from the release of inflammatory mediators such as histamine, causes an increase in vascular caliber and leads to an increase in blood flow which is responsible for redness and heat in the inflamed area; phase 2: the vascular dilation is quickly followed by an increase in the permeability of the microvasculature, leading to the extravasation of plasma fluid and proteins into the extravascular tissues; phase 3: this increase in permeability causes the erythrocytes to

become more concentrated in the blood, leading to an increase in blood viscosity - a condition known as stasis. As stasis develops, there is an accumulation of blood leukocytes (mainly neutrophils) in the vascular endothelium. Simultaneously, endothelial cells are activated by mediators produced at the infection site or sites of damaged tissue, which causes an increase expression of adhesion molecules. This allows leukocytes to adhere to the endothelium and then migrate into the interstitial tissue in order to reach the injury site; and phase 4: once on the injury site, phagocytic cells such as neutrophils, macrophages and dendritic cells, can ingest and eliminate microorganisms, foreign bodies and necrotic cells, contributing to the resolution of inflammation (Kumar et al., 2010; Serhan, 2010).

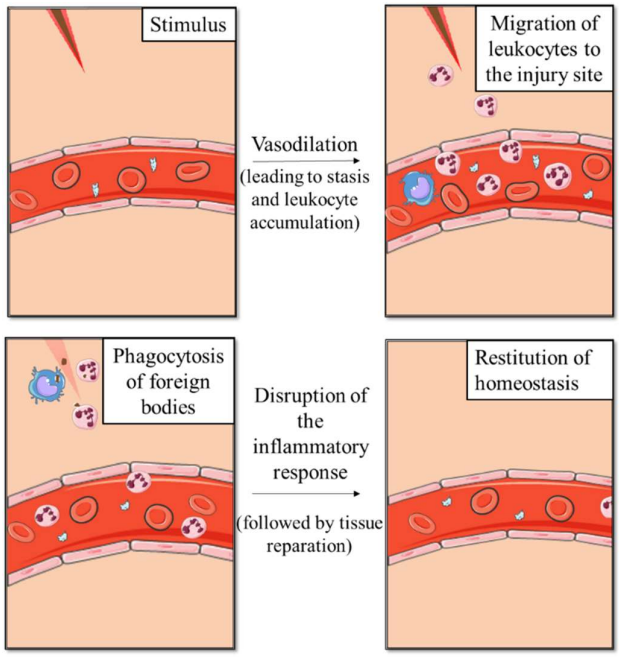

Figure 5. Schematic representation of main events of the inflammatory process. Figure made using the Servier Medical Art ("Powerpoint image bank | Servier,")

As early mentioned, the inflammatory process needs to be tightly regulated in order to prevent damage to healthy tissues. Inflammation is orchestrated by inflammatory mediators, that are only produced in short bursts while the pro-inflammatory stimulus persists, they have short half-lives, and are degraded after their release. Additionally, neutrophils have short half-lives outside the blood vessels and undergo apoptosis within a few hours in the tissues and as the inflammation develops there are a variety of stop signals which are triggered in order to terminate the process (Nathan, 2002; Serhan and Savill,

2005). These stop signals lead to the activation of mechanisms enabling a change in the arachidonic acid metabolites that are being produced, from pro-inflammatory metabolites (leukotrienes) to anti-inflammatory metabolites (lipoxins). In addition, these mechanism also lead to the release of anti-inflammatory cytokines, such as transforming growth factor-β (TGF-β) and interleukin-10 (IL-10), production of anti-inflammatory lipid mediators derived from polyunsaturated fatty acids (resolvins and protectins), and neural impulses that inhibit the production of tumor necrosis factor (TNF) by macrophages (Serhan et al., 2008; Tracey, 2002).

1.2.2 Immune players and inflammatory mediators in respiratory system

In the lungs, innate immune response is orchestrated by lung leukocytes, and epithelial cells of the alveolar and conducting airways surfaces (Martin, 2005). In general, the predominant leukocytes acting in the inflammatory response are the neutrophils in the first 6 to 24 hours being then replaced by monocytes in the subsequent 24 to 48 hours. These monocytes differentiate then into macrophages at the tissue level (Kumar et al., 2010).

As previously described, the inflammatory response also relies on soluble mediators, such as proteins and lipids, to help control the different stages of the inflammation. These mediators can be sorted according to their origin in two main groups: the cell-derived and the plasma protein-derived mediators. Among the cell derived mediators are included the vasoactive amines, the arachidonic acid metabolites, the reactive oxygen species (ROS), the nitric oxide, the platelet-activating factor (PAF), the cytokines and the chemokines. The plasma protein-derived group is composed by the mediators from the complement system, the coagulation system, and the kinin system (Kumar et al., 2010).

Among cell-derived mediators, histamine assumes a particular relevance in the inflammatory process in the respiratory system. It's produced mainly by mast cells that are present in connective tissue beneath the airway basement membrane (the bronchial lumen), near submucosal blood vessels and in the alveolar septa. Histamine is released in response to various stimuli (*e.g.* physical trauma) and causes bronchoconstriction, mucosal edema, and increased mucus secretion (Kumar et al., 2010; Martin, 2005). Another important group of inflammatory cell-derived mediators are the arachidonic acid metabolites, which includes the prostaglandins, leukotrienes, and lipoxins. Prostaglandins are produced mainly by mast cells, macrophages, and endothelial cells. These compounds result from the action of two

cyclooxygenases (COX), COX-1, which is constitutively expressed, and COX-2, which is inducible. The most important prostaglandins in the inflammatory response are the prostaglandins E_2, D_2, $F_{2\alpha}$, I_2. and thromboxane, deriving each one from the action of a different specific enzyme. Some of the effects of these compounds include: platelet aggregation and vasoconstriction (thromboxane), vasodilation (prostaglandins D_2 and I_2), inhibition of platelet aggregation and potentiation of the permeability-increasing and chemotactic effects of other mediators (prostaglandin I_2), contraction of bronchial smooth muscle and small arterioles (prostaglandin $F_{2\alpha}$), and chemoattraction of neutrophils (prostaglandin D_2) (Kumar et al., 2010; Ricciotti and FitzGerald, 2011; Serhan et al., 2008). The leukotrienes, on the other hand, are produced by the action of the lipoxygenase enzyme. The leukotrienes are mainly produced by leukocytes, acting as chemoattractants for these cells and having vascular effects. In particular, the leukotriene B_4 can act as a strong chemotactic agent and activator of neutrophils, leading to the aggregation and adhesion of the neutrophils to the venular endothelium, release of lysosomal enzymes, and generation of ROS. On the other hand, leukotrienes C_4, D_4, and E_4 can cause intense vasoconstriction, bronchospasm and augmented vascular permeability, being more potent than the histamine in the latter effects (Kumar et al., 2010; Serhan et al., 2008). Finally, the lipoxins are also formed through the action of the lipoxygenase. However, unlike the leukotrienes, lipoxins are inhibitors of the inflammation. Leukocytes, mainly neutrophils, produce intermediate compounds in the lipoxin synthesis, which are then converted to lipoxins by platelets. Lipoxins primarily act in the inhibition of leukocyte recruitment and neutrophil chemotaxis, and adhesion to the endothelium (Kumar et al., 2010; Serhan et al., 2008).

Another cell-derived mediator of the inflammatory cascade is PAF, which is produced by a range of different cells, such as platelets, basophils, mast cells, neutrophils, endothelial cells and alveolar macrophages. This mediator can cause platelet aggregation, vasoconstriction and bronchoconstriction and, in extremely low concentration, it can also cause vasodilation and augmented permeability in venules, with a higher strength than that of histamine (up to 10000 times higher). In addition to these effects, PAF also causes an increase in the leukocyte adhesion to the endothelium, oxidative burst, chemotaxis, and it can boost the synthesis of other inflammatory mediators, particularly eicosanoids (*e.g.* prostaglandins and leukotrienes) (Kumar et al., 2010; Stafforini et al., 2003).

Among the cell-derived mediators there are also soluble proteins, named cytokines, which are mainly produced by activated lymphocytes and macrophages and whose purpose is to modulate the functions of other cells. A few examples of this group of soluble proteins include, IL-1, IL-6, TNF, and chemokines. TNF and IL-1 are two of the major effectors of the inflammatory process, exerting both local and systemic effects. The local effects of these mediators have actions on three main cell types: vascular endothelium, leukocytes, and fibroblasts. At the vascular endothelium, TNF and IL-1 stimulate the expression of adhesion molecules, coagulation and production of IL-1 and chemokines, while suppressing the anticoagulant activity. These soluble proteins also activate leukocytes and stimulate the production of other inflammatory cytokines. Finally, TNF and IL-1 stimulate the proliferation of fibroblasts and collagen synthesis by these cells. As for the systemic effects of these mediators, they include fever, leukocytosis, loss of appetite, positive modulation of the production of acute-phase proteins, and stimulation of sleep (Kumar et al., 2010).

Chemokines, a family of small proteins, constitute another important player in the inflammatory process, acting mainly as chemoattractant for leukocytes. These molecules are distributed according to four groups: i) α chemokines (*e.g.* IL-8), which are released by macrophages and act on the activation and chemotaxis of neutrophils, with some activity on monocytes and eosinophils. The release of these chemokines is stimulated by microbial products and other cytokines (IL-1 and TNF); ii) β chemokines (*e.g.* monocyte chemoattractant protein, eotaxin), which are chemoattractant to monocytes, eosinophils, basophils and lymphocytes; iii) γ chemokines (*e.g.* lymphotactin), which are specific chemoattractant for lymphocytes; and iv) CX3C chemokines (*e.g.* fractalkine), which acts as a potent chemoattractant for monocytes and T cells in its soluble form, however in its cell-surface bound form, it promotes adhesion of monocytes and T cells (Charo and Ransohoff, 2006; Sallusto and Mackay, 2004).

Other important players in the inflammatory process are the reactive oxygen and nitrogen species (ROS and RNS, respectively). ROS are oxygen derived free radicals, mainly superoxide anion, hydrogen peroxide and hydroxyl radical, produced by leukocytes through the activation of the NADPH oxidase system. When released, these mediators increase the expression of chemokines, cytokines and leukocyte adhesion molecules, amplifying the inflammatory response. ROS are also the main effectors in the destruction of phagocytosed microbes. The release of high levels of these mediators can cause massive cell damage to the

host; to prevent these damages, the organism uses a series of antioxidant mechanisms (Kumar et al., 2010; Salvemini et al., 2006). Nitric oxide, produced by the activity of inducible nitric oxide synthase (NOS2), is also an important mediator of inflammation, and when present in high levels, it also acts as a microbicide agent (Cirino et al., 2006; Laroux et al., 2001).

Finally, among the plasma protein-derived mediators, the complement system mediators C3a, C5a, and C4a act on the inflammatory response by stimulating histamine release from mast cells. Moreover, C5a is also a strong chemotactic agent for neutrophils, eosinophils, monocytes and basophils, and activates the lipoxygenase pathway in neutrophils and monocytes. The C3b connects to microbial cell walls, promoting the phagocytosis by macrophages and neutrophils. In turn, the kinin mediator bradykinin, is responsible for increasing the vascular permeability, and causing systemic effects such as pain (Kumar et al., 2010).

Since the respiratory system is the primary and major exposure site to inhaled air particles, the toxicological study of their interaction is of great relevance, particularly in respect to possible pro-inflammatory effects. This topic is therefore explored in the following section.

1.2.3 Airways inflammation and oxidative stress due to inhalation of air particles

Understanding the interaction between the body and atmospheric air particles, as well as the mechanisms through which the air particles cause inflammation and oxidative stress is of major importance. One of the main theories that has been put forward is that particles lead to pro-inflammatory responses and other cellular effects by means of formation of ROS and induction of oxidative stress. However, there are also other mechanisms leading to the activation of non-oxidant pro-inflammatory mediators, such as the activation of channels, like the transient receptor potential cation channel subfamily V member 1 or TRPV1, directly by combustion particles (Øvrevik et al., 2015). Table 1 summarizes the main biological effects of the exposure to PM.

Table 1. Summary of the main biological responses to PM exposure

Experimental method	Sample	Main observations	Reference
In vitro study on rat alveolar cell lines	$PM_{2.5}$ and PM_{10}	• Oxidative stress induction due to the particle contents on Ni, Cr, Cu and WSOC.	(Daher et al., 2012)
In vitro study on macrophages	PM	• Dose dependent modulation of NO production due to alterations on NO synthase protein expression.	(Chauhan et al., 2004)
In vivo study on rats	$PM_{2.5}$	• Inflammation mediated by pathways regulated by ROS and NO. • Oxidative stress mainly due to inhibition of SOD activity. • Activation of metabolic enzymes leading to exacerbation of respiratory diseases.	(Li et al., 2015)
In vivo study on rats	Ambient and wood smoke air particles	• Oxidative stress induction. • Stimulation of pro-inflammatory genes in the lungs.	(Danielsen et al., 2010)
In vitro study on alveolar epithelial cells and macrophages	PM_{10}	• Cytotoxicity, pro-inflammatory response and oxidative stress induction. • When exposed in equal concentrations of rural and urban extracts; urban extracts produced a greater response.	(Michael et al., 2013)
In vitro study on human bronchial epithelial cells	Diesel exhaust particles	• Pro-inflammatory response through activation of NF-kB and MAPK pathways.	(Totlandsdal et al., 2010)
In vivo study on humans	Diesel exhaust particles	• Increased production of IL-8, endothelial adhesion molecules and neutrophil recruitment	(Stenfors et al., 2004)

Nowadays, there are several studies relating air particles inhalation and the induction of oxidative stress. Daher and co-workers, using rat alveolar cell lines, studied the redox activity of fine and coarse PM (Daher et al., 2012). The authors verified the existence of a strong correlation between cell ROS production and the PM content in Ni, Cr, Cu and WSOC, suggesting that these PM constituents are the main factors responsible for oxidative stress induction. Another recent *in vitro* study using macrophages, demonstrated that the capacity of PM to induce ROS is inversely correlated to PM size, and that photochemical aging as well as the content in Cu, Cr, Pb, Co, Ni and WSOC causes an increase in ROS production (Saffari et al., 2014). Chauhan and co-workers carried out an *in vitro* study to assess the effect of air particles in the nitric oxide production by macrophages (Chauhan et al., 2004). The authors reported that the exposure to inhalable air particles induce a dose dependent modulation of nitric oxide released, and concluded that this modulation was caused by an alteration in nitric oxide synthase protein expression (Chauhan et al., 2004). This set of studies suggest the potential of PM for inducing oxidative stress; however, beside the direct noxious effects of ROS and RNS, oxidative stress can also lead to the activation of a series of intracellular signaling pathways, such as MAPK transcription factors activator protein 1 (AP-1) and NF-kB. These signaling pathways control the expression of numerous pro-inflammatory effectors such as interleukins, COX-2, and inducible isoform of the nitric oxide synthase (NOS2), which are major players in pathological changes of the lungs (Li et al., 2008; Mazzoli-Rocha et al., 2010).

Beside the induction of oxidative stress, PM can also promote the production of pro-inflammatory mediators, leading to inflammation and damage of the airways. In an *in vivo* study on the effects of $PM_{2.5}$ on rats, Li and co-workers reported that $PM_{2.5}$ induced a lung inflammatory injury, accompanied by an increase in pro-inflammatory cytokine levels and inflammatory cell numbers (Li et al., 2015). The authors also verified that the oxidative stress caused by $PM_{2.5}$ was due to both the inhibition of the super oxide dismutase (SOD) activity and the stimulation of the iNOS activity, leading to an increase in the nitric oxide levels. The authors concluded that $PM_{2.5}$ induced inflammation in the rat lungs is mediated, in part, by the pathways mediated by ROS and nitric oxide and the activation of metabolic enzymes which exacerbate respiratory diseases (Li et al., 2015). Similarly, Danielsen and co-workers, using an *in vivo* study in rats, also verified that ambient and wood smoke air particles, induced an oxidative stress response and a stimulation of the expression of pro-inflammatory

genes in the lungs (Danielsen et al., 2010). Michael and co-workers, using an *in vitro* approach, verified that the cytotoxicity, oxidative stress, and pro-inflammatory responses in lung epithelial cells and macrophages significantly differed after exposure to equal concentrations of urban and rural PM, with the highest values being associated with urban air particles (Michael et al., 2013). This result confirms the hypothesis that PM composition and source constitute an important factor in PM-induced toxicity (Michael et al., 2013).

Additional studies have been reported in the literature focusing on both the effects of PM on the production of pro-inflammatory mediators, and in several pathways that play an important role in the immune system. In an *in vitro* study of the effects of DEP in human bronchial epithelial cells, Totlandsdal and co-workers reported that the pro-inflammatory response induced by DEP appeared to occur via both the activation of nuclear factor kB (NF-kB) and the p38 mitogen-activated protein kinase (MAPK) (Totlandsdal et al., 2010). Another *in vitro* study on the induction of cytokine expression in human bronchial epithelial cells by PM, showed an increase in the transcription of mRNA and the release of IL-1, IL-8, granulocyte-macrophage colony-stimulating factor, and leukemia inhibitory factor, leading to the enhancement of the inflammatory response in the lungs (Fujii et al., 2001). These results are corroborated by *in vivo* data showing that asthmatic and healthy humans exposed to DEP produce a vast profile of cytokines (Stenfors et al., 2004). According to this data, DEP had a direct effect on the IL-8 production, with an upregulation of endothelial adhesion molecules and neutrophil recruitment in healthy human airways, whereas the mildly asthmatic humans responded with an induction of epithelial IL-10 (Stenfors et al., 2004). The gathered data suggest that more work is required to clarify the different conclusions reported in the literature.

1.3. Objectives of the M.Sc. Thesis

The review presented in this Introduction section, has shown that atmospheric PM can have different chemical composition, depending on their local or regional sources, sampling location (i.e., remote, rural, or urban location and, therefore, linked to variations in residence time in the atmosphere), and even the seasonal period. It has been shown that the fine size range of PM, *i.e.*, $PM_{2.5}$, is composed mainly of EC, OC (consisting of a water-soluble and a water-insoluble fraction), water-soluble inorganic salts, mineral dust, and sea salt. Moreover, the $PM_{2.5}$ can exert an array of detrimental effects on the human health,

including the increasing risk of cardiovascular and pulmonary diseases, carcinogenic effects, oxidative damage to DNA, and effects on the immune system causing augmented susceptibility to infections and pathogens. In the airways, $PM_{2.5}$ is known to induce oxidative stress and inflammation (*e.g.* through stimulation of the production and release of pro-inflammatory mediators), leading in some cases to lung injury.

An important finding of this review work is that atmospheric $PM_{2.5}$ can have different effects on the lungs tissues depending on its chemical composition. The available literature on this issue suggests that water-soluble trace metals (*e.g.*, Ni, Cu, Cr, Co and Pb) and WSOC have an important influence on the oxidative potential of airborne PM. Nevertheless, it should also be highlighted that the link between WSOC composition and PM-induced oxidative activity is still unknown, mostly because of the complex nature of the atmospheric particulate WSOC component. Accurate characterization of the WSOC fraction is therefore mandatory for better understanding the effect of this organic fraction on PM-associated pro-inflammatory potential, particularly in urban areas.

Thus, the main objective of this M.Sc. thesis is to assess the pro-inflammatory effects and oxidative potential of the WSOC fraction from atmospheric aerosol samples. To these aims, $PM_{2.5}$ samples were collected at the campus of the University of Aveiro, which is classified as a near-city background site, located between 3 and 10 km from large pollution sources (*e.g.*, an industrial complex, which includes the production of nitric acid, aniline, nitrobenzene and chlorate compounds, is located 10 km to the North of the city of Aveiro). The sampling campaign was conducted during the day and night periods in late autumn, in order to assess and compare the role played by different ambient conditions on the effect of WSOC on the PM-associated oxidative potential. The WSOC fractions were extracted from the collected $PM_{2.5}$ samples following analytical procedures described in previous studies (*e.g.,* (Duarte et al., 2016)). The structural features of the collected aerosol WSOC fractions were assessed by means of excitation-emission matrix (EEM) fluorescence, ultraviolet-visible (UV-Vis), and solution-state one-dimensional ^{1}H nuclear magnetic resonance (NMR) and two-dimensional NMR (^{1}H-^{1}H Correlation Spectroscopy (COSY), and ^{1}H-^{13}C Heteronuclear Single Quantum Coherence (HSQC) and Heteronuclear Multiple Bond Correlation (HMBC)) spectroscopies. Finally, the biological effects of the WSOC fractions collected under the different ambient conditions were assessed on Raw 264.7 macrophage

cell line. The results were then related to the atmospheric concentrations and structural characteristics of the different WSOC fractions.

Chapter 2

Materials and Methods

2.1 Atmospheric aerosol sampling campaigns

The $PM_{2.5}$ samples were collected on pre-fired (at 500 °C for 12h) quartz fibre filters (20.3 × 25.4 cm Whatman QM-A) with an airflow rate of 1.13 m^3 min^{-1}. The high-volume sampler (model TE-6070V, Tisch Environmental, Inc.) was provided with a pre-separator for excluding particles larger than 2.5 μm. This size-cut was accomplished using a size selective PM_{10} inlet (model TE-6001, Tisch Environmental, Inc.) and a $PM_{2.5}$ single-stage impactor (model TE-231, Tisch Environmental, Inc.) and a back-up quartz filter. The total mass of the collected $PM_{2.5}$ samples was determined by weighing the filter under controlled moisture conditions before and after sampling. The filters were then wrapped with aluminium paper and stored frozen until further analysis.

The sampling campaign was conducted between the 14th and 29th of November 2016 (late autumn), during the weekdays (*i.e.*, from Monday to Friday) and in two distinct time periods: (i) day-time: 9:40 a.m. to 5:30 p.m. and (ii) overnight: 5:40 p.m. to 9:30 a.m. Throughout the sampling period no attempts were made to control any adsorption/desorption phenomena on the filters. Consequently, some volatilisation/condensation processes may occur on the filter and particles surface for semi-volatile organics. Also, oxidation by strong oxidants (e.g. ozone) of filter deposited organics may occur during aerosol collection. Therefore, in a similar fashion to what has been considered in previous works ((Duarte et al., 2007; Lopes et al., 2015), the measured concentrations and chemical features for oxygenated organic species, namely WSOC, should be considered an upper limit of the true atmospheric levels.

2.2. Extraction of aerosol WSOC fractions

An area of 315 cm^2 of each filter was extracted with 150 mL of ultra-pure water (18.2 M Ω cm, filter area to water volume ratio of 2.1 cm^2 mL^{-1}) by mechanical stirring during 5 min plus ultrasonic bath during 15 min. The final slurry obtained was filtered through a hydrophilic polyvinylidene fluoride (PVDF) membrane filter (Durapore®, Millipore, Cork, Ireland) of 0.22 mm pore size. The filtered aqueous extracts were then collected into vials and stored frozen until further analysis.

2.3. Excitation–emission matrix (EEM) fluorescence spectroscopy of the WSOC samples

The fluorescence spectra of each WSOC sample were recorded on a spectrophotometer JASCO (Tokyo, Japan) model FP-6500 using a 1 cm path-length quartz cuvette. Excitation and emission wavelength ranges were set from 220 to 450 nm and 250 to 600 nm, respectively, and their scanning intervals were set at 10 nm and 5 nm, respectively. The excitation and emission slit widths were fixed at 10 nm and the scan speed was set at 100 nm min^{-1}. For each day of EEM analysis, a spectrum of ultra-pure water was acquired under the same experimental conditions and used as blank. The peaks due to water Raman scattering were eliminated from all WSOC samples spectra by subtracting the ultra-pure water blank spectra.

2.4. UV-vis spectroscopy of the WSOC samples

The UV–vis spectra (in the range of 200–600 nm) were registered on an UV–vis spectrophotometer Shimadzu (Dusseldorf, Kent, Germany) Model UV 2101PC in 2 cm path length quartz cells. Ultra-pure water was used as a blank.

2.5. Dissolved Organic Carbon (DOC) analysis of the WSOC samples

The DOC content of the aqueous extracts of the $PM_{2.5}$ samples was measured by means of a Skalar (Breda, Netherlands) San++ Automated Wet Chemistry Analyzer, based on a UV-persulfate oxidation method (Lopes et al., 2006). The WSOC concentrations are expressed in μg C m^{-3}.

2.6. WSOC samples preparation for NMR and biological studies

In order to have sufficient amount of WSOC samples for both NMR structural characterization and biological assay studies, the WSOC samples from each daily time period were batched together, on a total of two pooled WSOC samples representative of Day and Night time conditions. Subsequently, each pooled WSOC sample was concentrated in a rotary evaporator, at 35ºC, until a final volume of approximately 200 mL. This volume was equally separated (100 mL) into 2 round-bottom flasks (one for NMR analysis and the other

for the biological assays), which were then freeze-dried and kept on a dessicator over silica gel.

2.7. 1D and 2D NMR spectroscopy

All NMR spectra were acquired using a Bruker Avance-500 spectrometer operating at 500.13 and 125.77 MHz for ^{1}H and ^{13}C, respectively, equipped with a liquid nitrogen cooling CryoProbe. The dried WSOC samples (7-3 mg) were dissolved in deuterated methanol (MeOH-d_4, approximately 1 mL) and transferred to 5mm NMR tubes. All 1D ^{1}H NMR spectra were run at 22 °C, under the following conditions: i) pulse with of 10.8 μs; b) acquisition time of 2.97 s; c) 65 k data points; d) spectral with of 11029 Hz; e) recycle delay of 1 s; and f) 512 scans. A suppression pulse sequence was also applied to eliminate the water signal interference (≈ δ ^{1}H 5 ppm). The identification of functional groups in the NMR spectra was based on their chemical shift relative to that of an external tetramethylsilane (TMS) standard set at 0.0 ppm.

The 2D NMR spectra were run under the following conditions: i) *g*COSY spectrum was recorded with 156 transients over 170 increments (zero-filled to 1K) and 2K data points with spectral widths of 5000 Hz. The recycle delay was 1 s. The data were processed in the absolute value mode; (ii) the phase sensitive ^{1}H-detected (^{1}H,^{13}C) *g*HSQC spectrum was recorded with 140 transients over 154 increments (zero-filled to 1K) and 2K data points with spectral widths of 5000 Hz in F2 and 22700 Hz in F1. The recycle delay was 1.5 s. A cosine multiplication was applied in both dimensions. The delays were adjusted according to a coupling constant $^{1}J_{CH}$ of 149 Hz; iii) the *g*HMBC spectrum was recorded with 188 transients over 197 increments (zero-filled to 1K) and 2K data points with spectral widths of 5000 Hz in F2 and 29000 Hz in F1. The recycle delay was 1.5 s. A sine multiplication was applied in both dimensions. The low-pass J-filter of the experiment was adjusted for an average coupling constant $^{1}J_{CH}$ of 149 Hz and the long-range delay utilized to excite the heteronuclear multiple quantum coherence was optimized for 7 Hz.

2.8 Cell culture

Raw 264.7, a mouse leukaemic monocyte macrophage cell line from American Type Culture Collection (ATCC number: TIB-71), was cultured in DMEM supplemented with 10% non-inactivated fetal bovine serum, 100 U mL^{-1} penicillin, and 100 μg mL^{-1} streptomycin at 37 °C in a humidified atmosphere of 95% air and 5% CO_2. Cells were routinely inspected for morphological changes by microscope observation and subcultured every two days until passage 30.

2.9 Cell viability assays

Cell viability was assessed by resazurin assay (O'Brien et al., 2000). Briefly, $0.05x10^6$ cells/well in a 96 well plate, were exposed to indicated concentrations of WSOC atmospheric fractions during 24h. Two hours before the end of exposure, resazurin solution was added to each well to a final concentration of 50 μM. Absorbance was then read at 570 and 600 nm in a Synergy microplate reader (Biotek, Winooski, VT, USA).

2.10 Nitric oxide production

The production of NO was measured by the accumulation of nitrite in the culture supernatants, using a colorimetric reaction with the Griess reagent. The cells were plated at 0.03×10^7 cells/well in 48-well culture plates, allowed to stabilize for 12h and then incubated with indicated concentrations of the WSOC. In some experiments, we address if exposure to extracts affects the capacity of macrophages to answer to strong pro-inflammatory stimuli such as bacterial LPS. For this, 1 μg mL^{-1} LPS was added following 1h exposure to extracts and cells incubated for 24h. For NO measurement, 100 μL of culture supernatants were collected and added to 100 μL of Griess reagent (0.1% (w/v) N-(1-naphthyl) ethylenediamine dihydrochloride and 1% (w/v) sulfanilamide containing 5% (w/v) H_3PO_4) for 30 minutes, in the dark. The absorbance at 550 nm was measured using a Synergy HT spectrophotometer.

2.11 Evaluation of NO Scavenging activity

The NO scavenging activity of WSOC was evaluated using S-nitroso-N-acetylpenicillamine (SNAP) as NO donor. Different concentrations of WSOC and SNAP (300 μM) were added to culture medium and maintained in a humidified incubator at 37 ºC for 6h. The medium was collected and the nitrite levels were determined by Griess reaction, as described above.

2.12 *In vitro* antioxidant activity

The potential antioxidant activity of WSOC was addressed by its capacity to prevent LPS-induced oxidative stress in macrophages. Briefly, Raw cells were plated at $0.05x10^6$ per well in a μ-Chamber slide (IBIDI GmbH, Germany), allowed to stabilize overnight and then stimulated with 1 μg mL^{-1} LPS during 16h. WSOC extracts were added 1h prior to LPS stimulation. At the end of incubation period cells were washed three times with HBSS (in mM: 1.3 $CaCl_2$, 0.5 $MgCl_2$, 5.3 KCl, 138 NaCl, 0.44 KH_2PO_4, 4.2 $NaHCO_3$, and 0.34 Na_2HPO_4, pH 7.4) and then loaded with 5 μM H_2DCFDA and 0.50 μg mL^{-1} Hoechst in HBSS for 30 min at 37 ºC in the dark. Cells were washed three times with HBSS, and analyzed with an Axio Observer Z1 fluorescent microscope (Zeiss Group, Oberkochen, Germany) at 63X magnification.

2.13 Analysis of gene expression by q-PCR

After cell treatment for the indicated times, total RNA was isolated with TRIzol reagent according to the manufacturer's instructions. The RNA concentration and possible contamination were assessed by OD260 measurement using a NanoDrop spectrophotometer (Thermo Scientific, Wilmington, DE, USA) and samples were stored in RNA Storage Solution (Ambion, Foster City, CA, USA) at -80 °C until use. Briefly, 1 μg of total RNA was reverse-transcribed using the iScript Select cDNA Synthesis Kit and real-time quantitative PCR (qPCR) reactions were performed using SYBR Green on a Bio-Rad CFX Connect (Bio-Rad, Hercules, CA, USA). After amplification, the fluorescence threshold was calculated using the CFX Manager software and the results normalized using *Hprt1* as reference gene. The final comparison of transcript ratios between samples was calculated by relative quantification method corrected for specific primer efficiencies. Primer sequences were designed using Beacon Designer software version 8 (Premier Biosoft International, Palo Alto, CA, USA) and thoroughly tested.

2.14 Analysis of NF-κB activation by immunofluorescence

To address the effects of WSOC extracts on the activation of NF-κB pathway, we analyzed its translocation to nucleus following exposure. For this, Raw cells were plated at $0.05x10^6$ per well in a μ-Chamber slides, allowed to stabilize overnight and then stimulated with 1 μg mL^{-1} LPS as positive control or with WSOC extracts during 30 min. In certain experiments, cells were exposed to WSOC extracts during 1h prior stimulation with LPS. This allow us to address possible inhibitory effects of the extracts on the NF-κB translocation promoted by LPS. After exposure, cells were fixed with 4% paraformaldeide during 15 min, washed twice with PBS and then permeabilized with 0.1% Triton X-100 in PBS containing 200 mM glycine during 10 min. Cells were then blocked for 1h at room temperature with 1% BSA in PBS. The slides were incubated overnight at 4 ºC with rabbit anti p65 NF-κB antibody (Cell Signaling, Danvers, MA, USA) diluted 1:100 in PBS 0.1% BSA. After 3 washing steps, cells were incubated with Alexa Flúor 555 Phalloidin (1:200) and anti-rabbit Alexa Fluor 488 secondary antibody (1:400) (both from Invitrogen Paisley, UK) during 1h at room temperature in the dark. Finally, the slides were washed 3 times with PBS, stained with DAPI (Invitrogen, Paisley, UK) during 2 min and then mounted with anti-fading mounting medium. The images were obtained with an Axio Observer Z1 fluorescent microscope (Zeiss Group, Oberkochen, Germany) at 63X magnification.

2.15 *In chemico* antioxidant activity

The *in chemico* antioxidant activity of WSOC was assessed by its capacity to directly scavenge ROS using the 2,2-diphenyl-1-picrylhydrazyl (DPPH) assay. Different concentrations of WSOC (1 mg mL^{-1} and 0.5 mg mL^{-1}) were added to a solution of DPPH incubated at room temperature in the dark for 20 minutes. After incubation OD was measured at 517 nm and scavenging activity of ROS was calculated based on a control solution of DPPH.

2.16 Statistical analysis

Comparisons between multiple groups (control vs conditions or LPS vs conditions) were performed by One-Way ANOVA analysis with a Dunnet´s post-test. Analysis of the differences between the LPS group and the ATM+LPS was performed by an unpaired

Student's *t* test. Statistical analysis was performed using GraphPad Prism, version 6 (GraphPad Software, San Diego, CA, USA).

Chapter 3

Structural characterization and biological effects of aerosol organic matter

3.1 Diurnal trend of fine urban aerosol and its WSOM fraction

In order to assess the diurnal trends of the fine urban aerosol and its WSOM fraction, the daily concentrations of $PM_{2.5}$ were calculated. Figure 6 shows the atmospheric concentrations of $PM_{2.5}$ samples collected during the sampling campaign. Overall, the night periods were characterized by higher $PM_{2.5}$ concentrations than those of daytime. Interestingly, the $PM_{2.5}$ concentrations are lower at the beginning of the week (Monday - 14th and 21st November -, and Tuesday - 15th and 22nd November), which might be associated with a low traffic rate during these days.

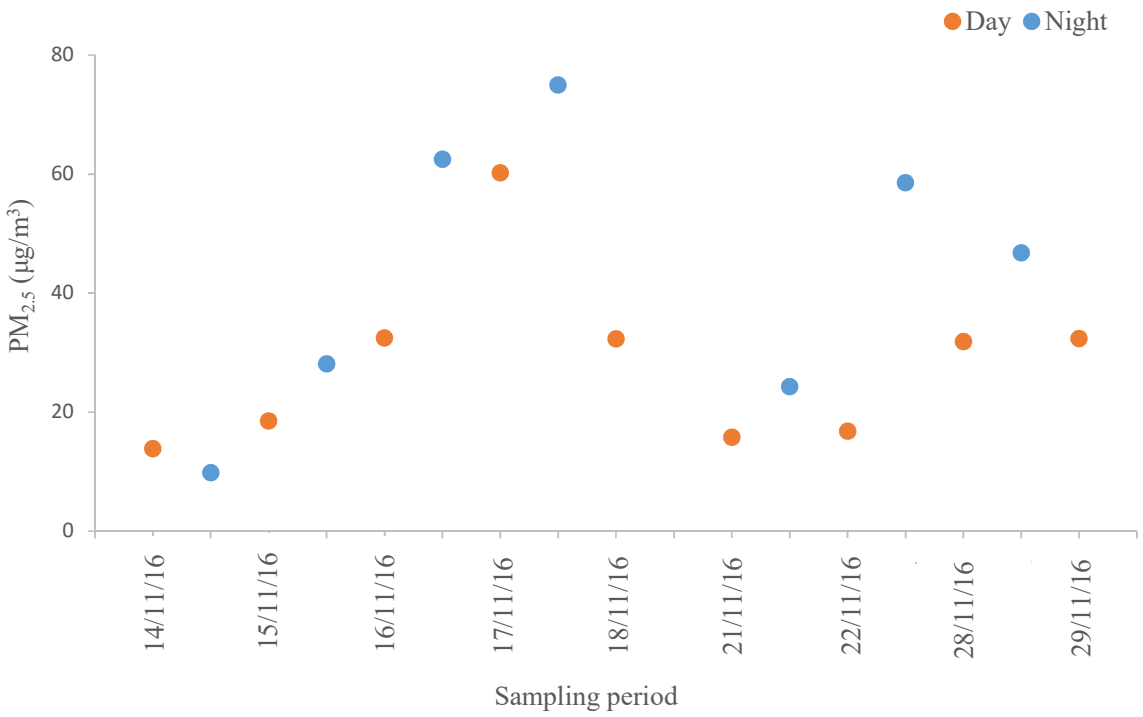

Figure 6. Atmospheric concentrations of $PM_{2.5}$ collected during the sampling campaign

The $PM_{2.5}$ samples collected during day time periods exhibit lower WSOC concentrations (median: 1.3 µg C m^{-3}; range: 0.19 to 5.6 µg C m^{-3}) than those collected during the night periods (median: 4.7 µg C m^{-3}; range: 0.51 to 6.5 µg C m^{-3}). These differences suggest the presence of a nighttime WSOC source, which alongside low air temperatures (see Table 1A, in Annexes), favors the particulate phase during this period (Jaiprakash et al., 2017). The WSOC concentrations were also used to estimate the

atmospheric concentrations of WSOM by applying a conversion factor of 1.6 (WSOM = WSOC x 1.6) established for the city of Aveiro (Duarte et al., 2015). Figure 7 shows the percentage of the WSOM component in the $PM_{2.5}$ samples. In the studied sampling periods, the WSOM accounts for an average of 9.2 ± 4.2% (2.0-15%) and 14 ± 3.3% (8.3-18%) of the $PM_{2.5}$ collected during day and night, respectively. The highest amounts of WSOM in the night period alongside the higher $PM_{2.5}$ concentrations could be explained by the temperature inversion and the lowering of the atmospheric mixing height, leading to a confinement of the air particles closer to the ground (Jaiprakash et al., 2017).

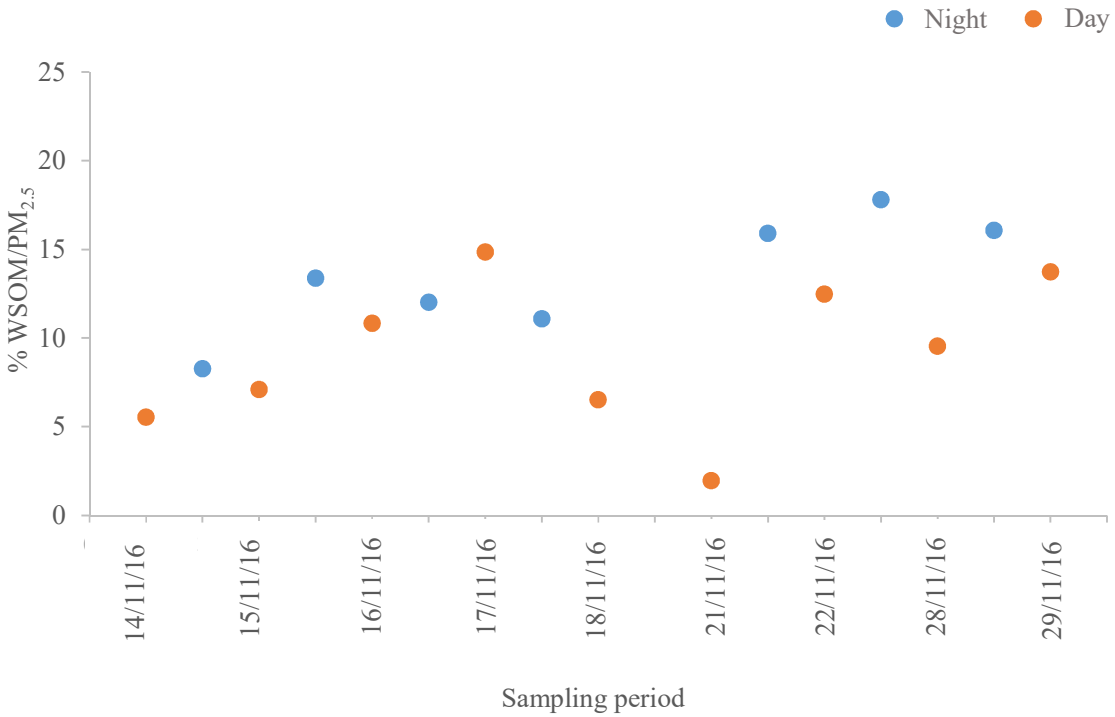

Figure 7 – WSOM content in PM2.5 total mass collected in each sampling period

3.2 Spectroscopic characterization of atmospheric aerosol WSOM samples

Figure 8 shows the EEM spectra of two fine aerosol WSOM samples collected during day and overnight. These EEM spectral profiles are representative of those obtained for the other WSOM samples (shown in Annexes – Figures A2 to A10). Indeed, no particular difference between samples was observed, other than fluorescence intensity as a result of higher WSOM concentrations in the night samples. All EEM spectra exhibit two main peaks

at different excitation and emission wavelengths (λ_{Exc} / λ_{Em}): 240/410 nm and 310/410 nm. Similar EEM spectra profiles have already been identified in the literature for urban aerosol WSOM samples, and they were associated with the presence of conjugated and/or aromatic compounds similar to those reported for the so-called "humic-like substances" (Chen et al., 2016a, 2016b; Matos et al., 2015).

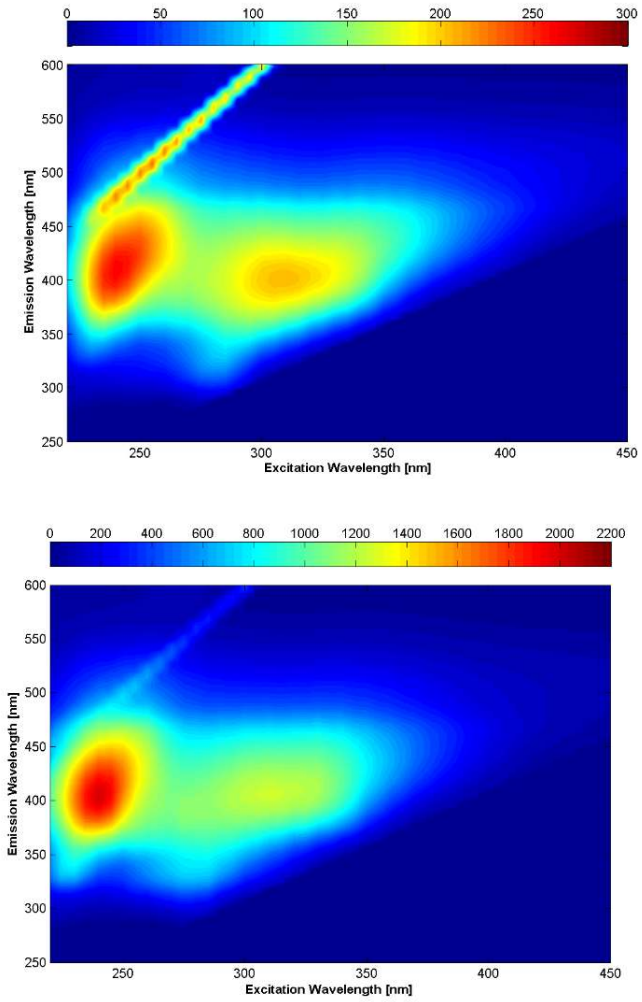

Figure 8. EEM fluorescence spectra of the aerosol WSOM samples collected in different time periods: day (up, 16/11/16) and night (down, 16/11/16 to 17/11/16)

The UV-visible spectrum of each aerosol aqueous extract (Figure A1, in the Annexes) was also very similar for all samples, decreasing monotonically with increasing wavelength. Little information can be drawn from such spectra, but through the examination of the quotient E_{250}/E_{365} (absorbances at 250 and 365 nm) some qualitative information can be

made. Figure 9 shows the obtained results for the ratio E_{250}/E_{365} for all aerosol WSOM fractions. In general, the E_{250}/E_{365} ratios are larger for samples collected during the night period, which is representative of a shifting in UV–vis absorbance towards low wavelengths associated with a lower degree of condensation of the WSOM (Duarte et al., 2005).

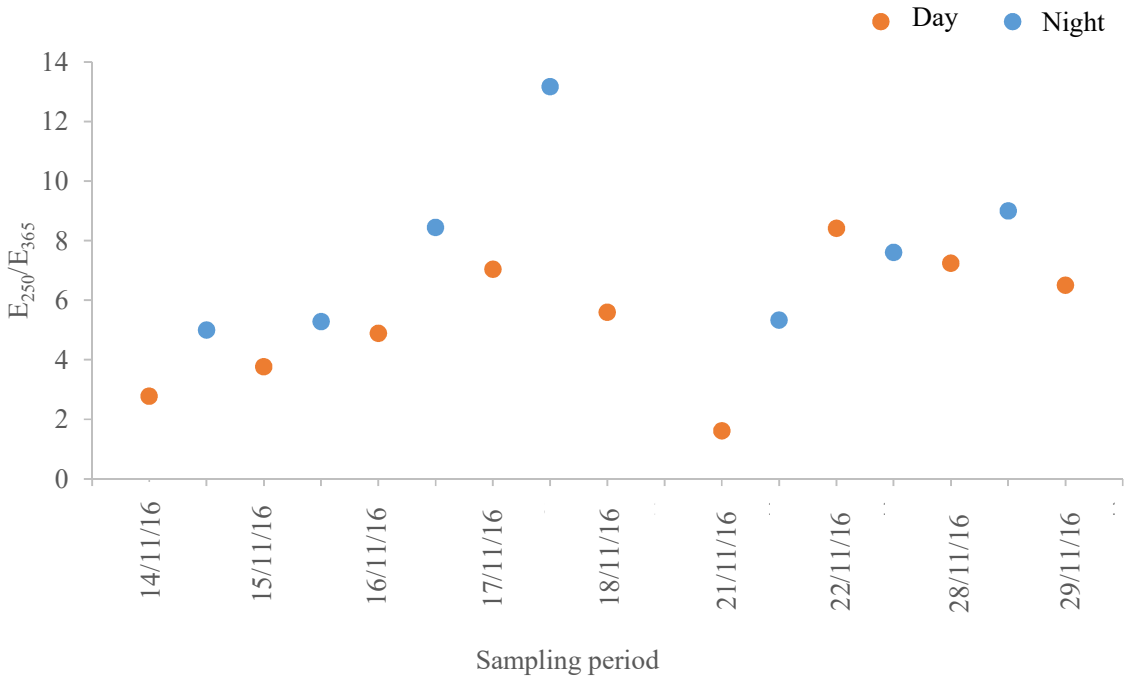

Figure 9 – E_{250}/E_{365} ratios of the WSOM extracts from $PM_{2.5}$ collected during the sampling campaign

Figures 10 and 11 present the solution-state ^1H NMR spectra of the WSOM extracted from fine aerosol samples collected during day and night time periods, respectively. Overall, all ^1H NMR spectra comprises a complex overlapping profile with broad bands superimposed by a relatively small number of sharp peaks. Although the characterization of specific individual organic species becomes difficult, four main categories of functional groups carrying C–H bonds can be identified: (i) δ ^1H 0.5–1.9 ppm – protons bound to carbon atoms of straight and branched aliphatic chains (H–C), which includes protons from methyl (R–CH_3), methylene (R–CH_2), and methyne (R–CH) groups; (ii) δ ^1H 1.9–3.2 ppm – protons bound to carbon atoms in α–position to unsaturated groups in allylic (H–C_α–C=), carbonyl or imino (H–C_α–C=O or H–C_α–C=N) groups, and protons in secondary and tertiary amines (H–C=NR_2 and NR_3); (iii) δ ^1H 3.3–4.1 ppm – protons bound to oxygenated saturated

aliphatic carbon atoms (H–C–O) in alcohols, polyols, ethers, esters, and organic nitrate (R–CH_2–O–NO_2), and (iv) δ ^{1}H 6.5–8.3 ppm – protons bound to aromatic carbon atoms (H–Ar), although alkenes protons in conjugated systems can also resonate within this chemical-shift range. For a further understanding of the ^{1}H NMR data, a quantitative integration of each spectral region was performed in order to assess the abundance of each functionality in the WSOM samples.

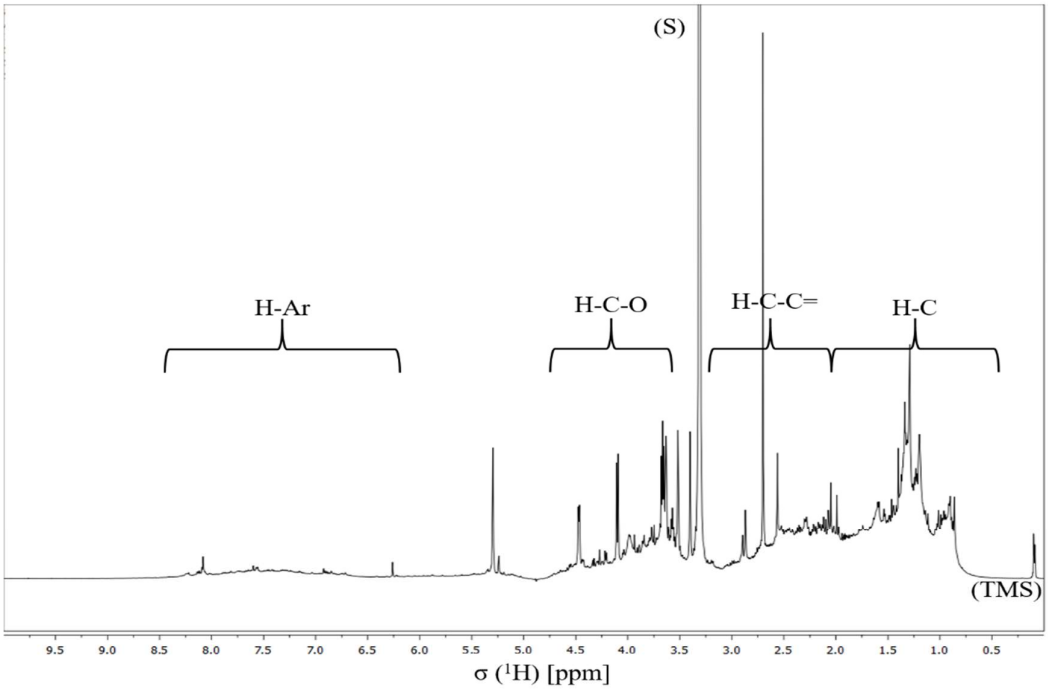

Figure 10. ^{1}H NMR spectrum of aerosol WSOM collected during day periods. Four spectral regions are identified at the top of the spectrum: H-C, H-C-C=, H-C-O, and Ar-H. Resonance signals: Solvent (S) – MeOH-d4, and Tetramethylsilane (TMS) - 0.03% (v/v)

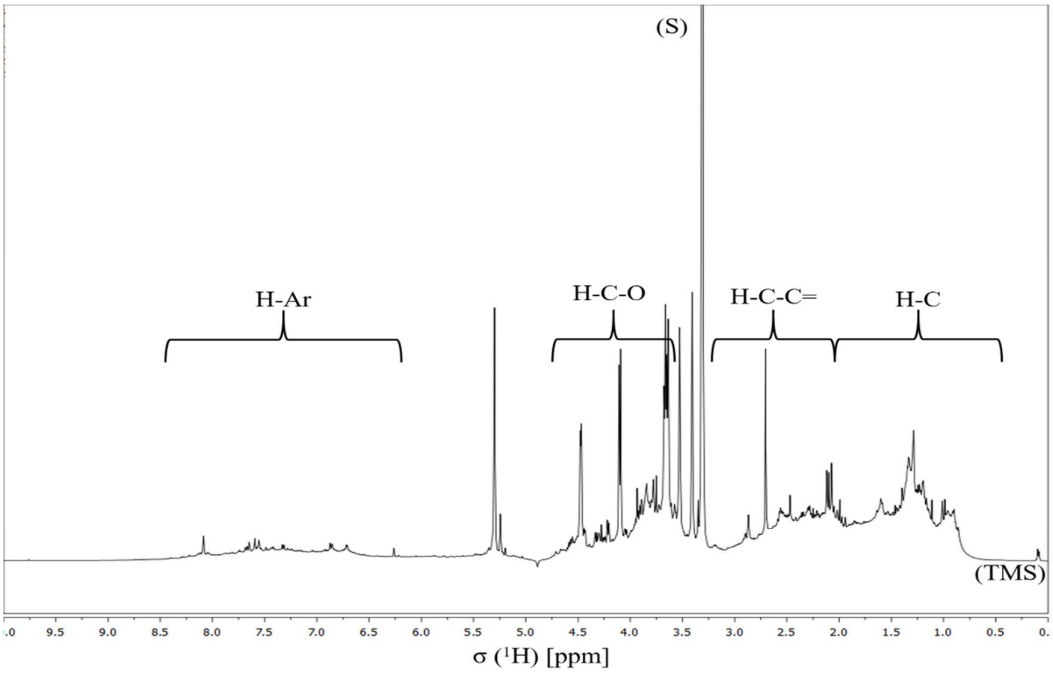

Figure 11. [1]H NMR spectrum of the aerosol WSOM collected during night periods. Four spectral regions are identified at the top of the spectrum: H-C, H-C-C=, H-C-O, and Ar-H. Resonance signals: Solvent (S) – MeOH-d4, and Tetramethylsilane (TMS) - 0.03% (v/v)

Figure 12 shows the percentage distribution of [1]H for the WSOM samples from fine urban aerosols collected during the day and night time periods. Integrated regions for WSOM showed a similar [1]H NMR profile as those reported in previous studies (*e.g.* (Decesari et al., 2000; Lopes et al., 2015; Tagliavini et al., 2006)). In these samples, the saturated aliphatic protons are the most important component, followed by unsaturated and oxygenated aliphatic protons, and a less contribution from aromatic protons. The aliphatic structures exhibit a distinct maximum (43%) in the day WSOM sample and a minimum (31%) in the overnight WSOM sample. Additional differences between the day and night WSOM samples are found in the spectral region associated with protons bound to oxygenated aliphatic (H–C–O) and aromatic (H–Ar) structures. The overnight WSOM sample show higher relative peak areas in these two regions (34% and 9%, respectively) than that collected during the day (24% and 5%, respectively). These spectral features suggest that the night WSOM sample might be enriched in organic structures resembling lignin- and carbohydrate-like compounds typically released from wood-burning processes from house heating during low temperature conditions (Duarte et al., 2015, 2008; Fine et al., 2001; Lopes et al., 2015; Paglione et al., 2014). As shown in Table A1 (in Annexes), the median of air temperature

during the night sampling period was approximately 4ºC lower than that observed during the day, being therefore very likely the use of domestic fireplaces for wood burning during this sampling period.

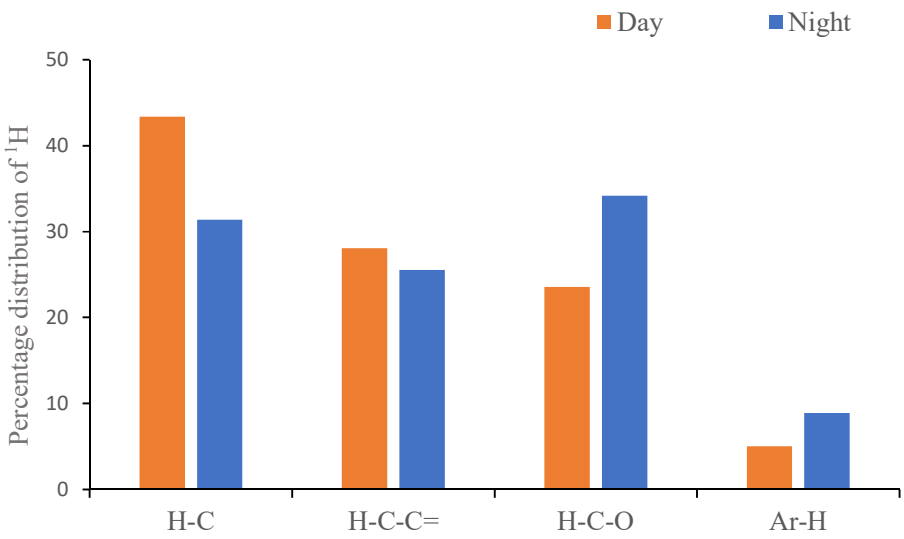

Figure 12. Percentage distribution of the ^{1}H functional groups in aerosol WSOM samples collected during the day and night time periods.

In this work, a range of 2D NMR techniques (namely ^{1}H-^{1}H COSY, ^{1}H-^{13}C HSQC, and ^{1}H-^{13}C HMBC) were also applied to further decode the structural features of the WSOM samples Figures 13 and 17 show the HSQC spectra of the day and night WSOM samples, respectively. The COSY and HMBC spectra of both samples are provided in section A4, in Annexes (Figures A11 to A14). The HSQC NMR spectra of the two WSOM samples reveal several important ^{1}H-^{13}C correlations in three major regions of chemical environments, but with very different relative intensities: aliphatic (δ ^{1}H 0.4 – 3.6 ppm / δ ^{13}C 10 – 45 ppm, including also *N*-alkyl groups at δ ^{1}H 2.6 – 3.6 ppm / δ ^{13}C 35 – 42 ppm), oxygenated aliphatic (δ ^{1}H 3.6 – 6.0 ppm / δ ^{13}C 50 – 107 ppm), and aromatic (δ ^{1}H 6.5 – 8.5 ppm / δ ^{13}C 107 – 160 ppm) regions. The distribution of the 2D NMR cross peaks across these three chemical shift areas are consistent with other 2D NMR spectral profiles found in literature related to WSOM fractions from field aerosol samples (Duarte et al., 2008; Matos et al., 2017; Schmitt-Kopplin et al., 2010) or laboratory experiments (Griffith et al., 2013; Maksymiuk et al., 2009). These regions were studied in more detail in an attempt to portray

the most important substructural fragments in both WSOM samples. Figures 14 to 16 show respectively the expanded aliphatic, oxygenated aliphatic, and aromatic regions of the ^{1}H-^{13}C HSQC spectrum of the WSOM sample collected during day time period, with some tentative structure assignments based on previously published data (Matos et al., 2017). In a similar fashion, Figures 18 to 20 depict the same aforementioned regions for the WSOM sample collected during the night period.

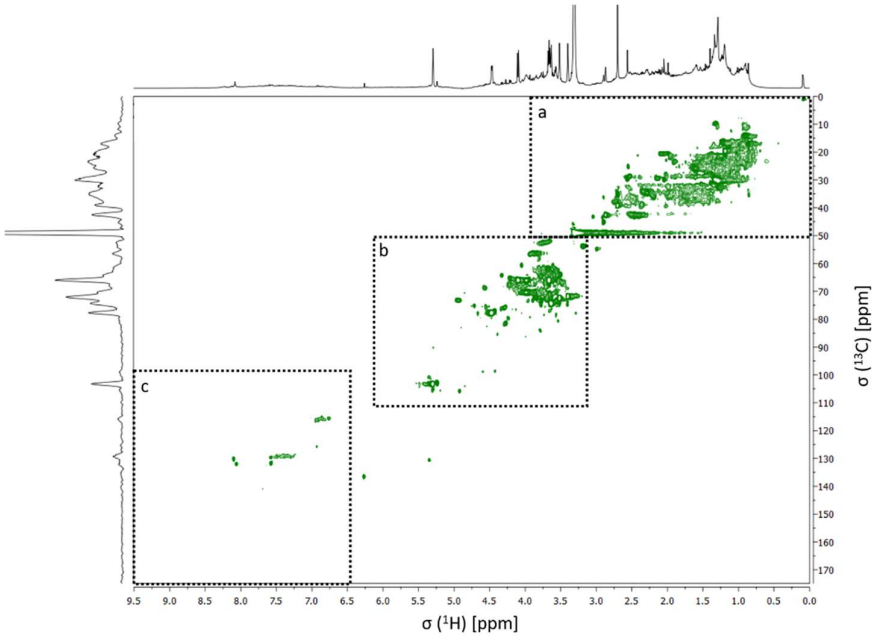

Figure 13. ^{1}H-^{13}C HSQC spectrum of the WSOM sample collected during day time period. Section A: aliphatic region; Section B: oxygenated aliphatic region; Section C: aromatic region;

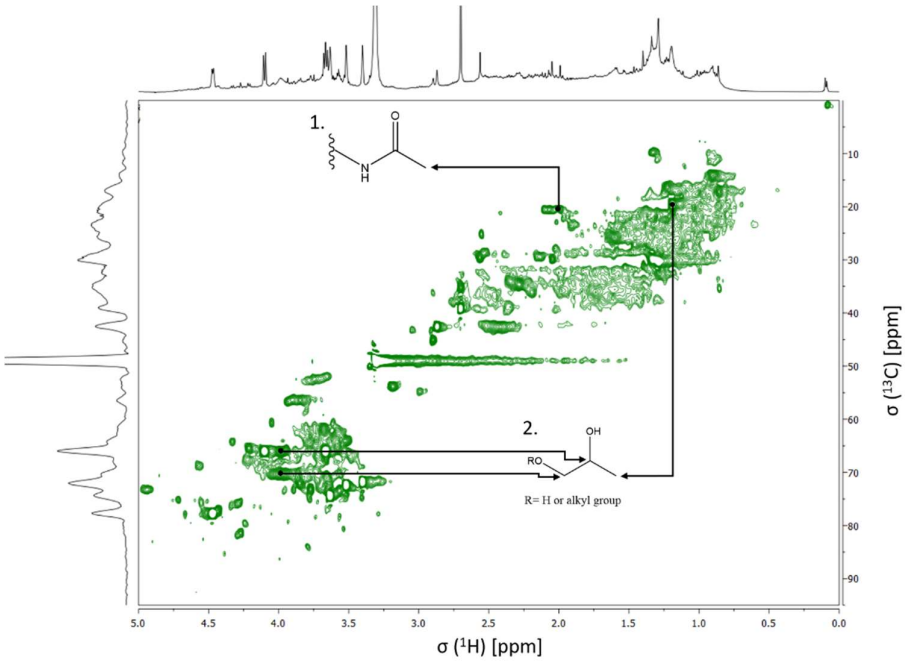

Figure 14. Expanded aliphatic region of the ^{1}H-^{13}C HSQC spectrum of the WSOM sample collected during day time periods, with some tentative structure assignments

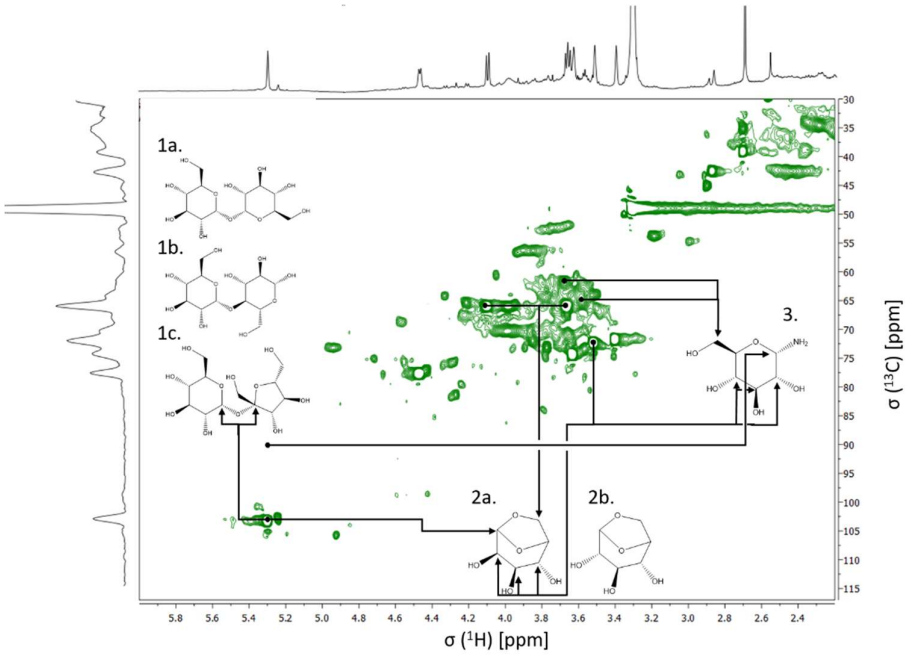

Figure 15. Expanded oxygenated aliphatic region of the ^{1}H-^{13}C HSQC spectrum of the WSOM sample collected during day time periods, with some tentative structure assignments

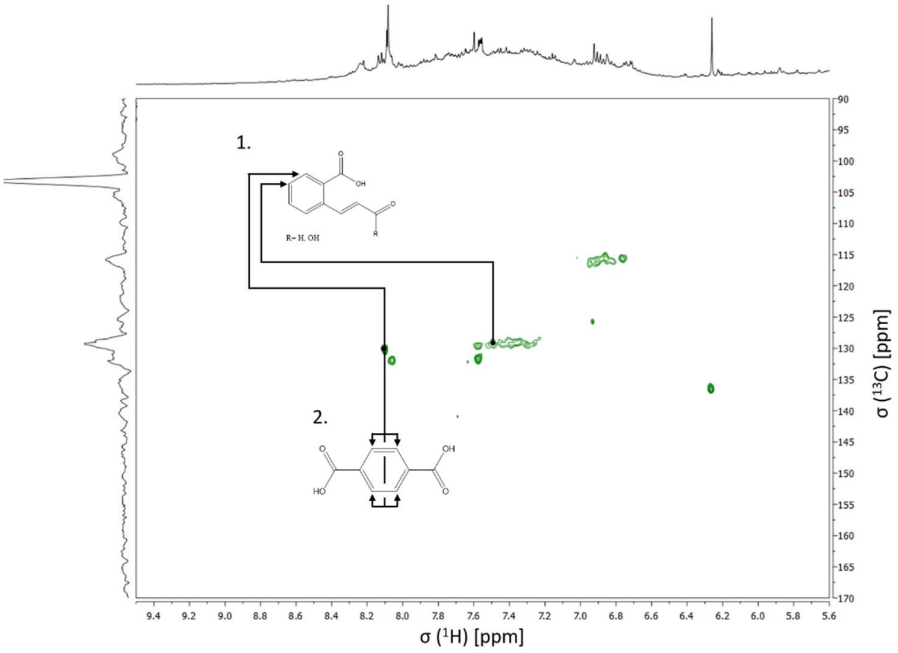

Figure 16. Expanded aromatic region of the ^{1}H-^{13}C HSQC spectrum of the WSOM sample collected during day time periods, with some tentative structure assignments

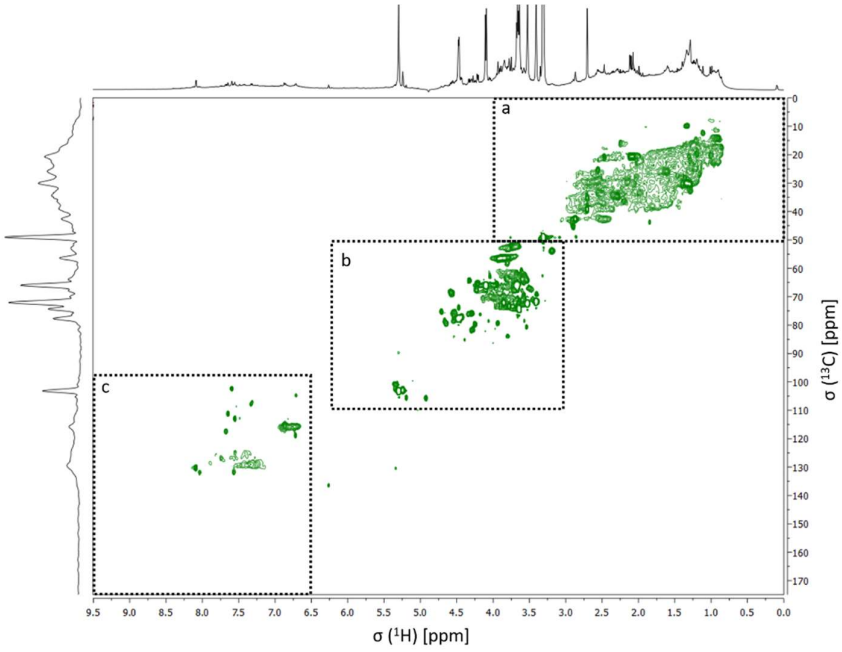

Figure 17. ^{1}H-^{13}C HSQC spectrum of the WSOM sample collected during night time periods. Section A: aliphatic region; Section B: oxygenated aliphatic region; Section C: aromatic region;

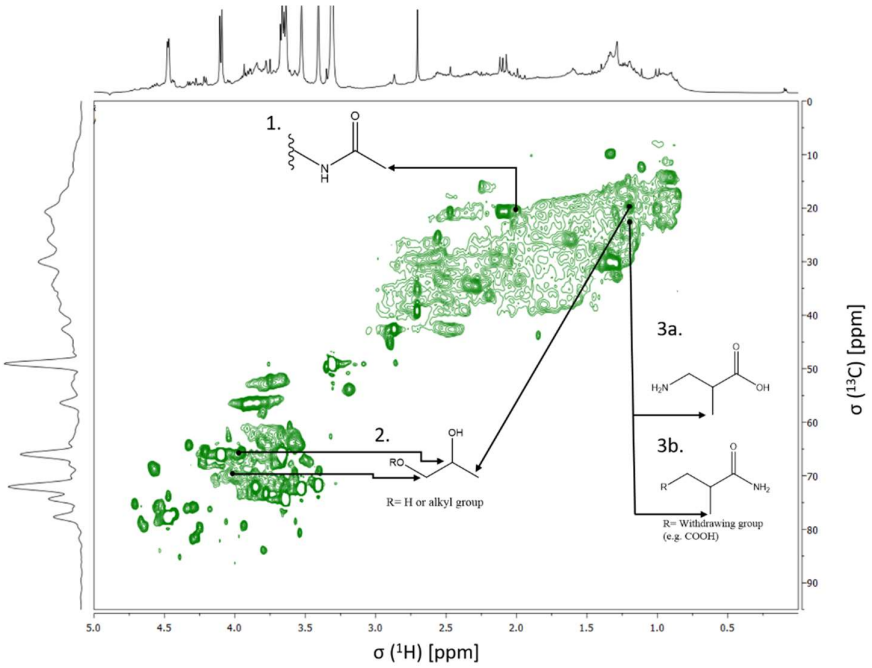

Figure 18 – Expanded aliphatic region of the ^{1}H-^{13}C HSQC spectrum of the WSOM sample collected during night time periods, with some tentative structure assignments

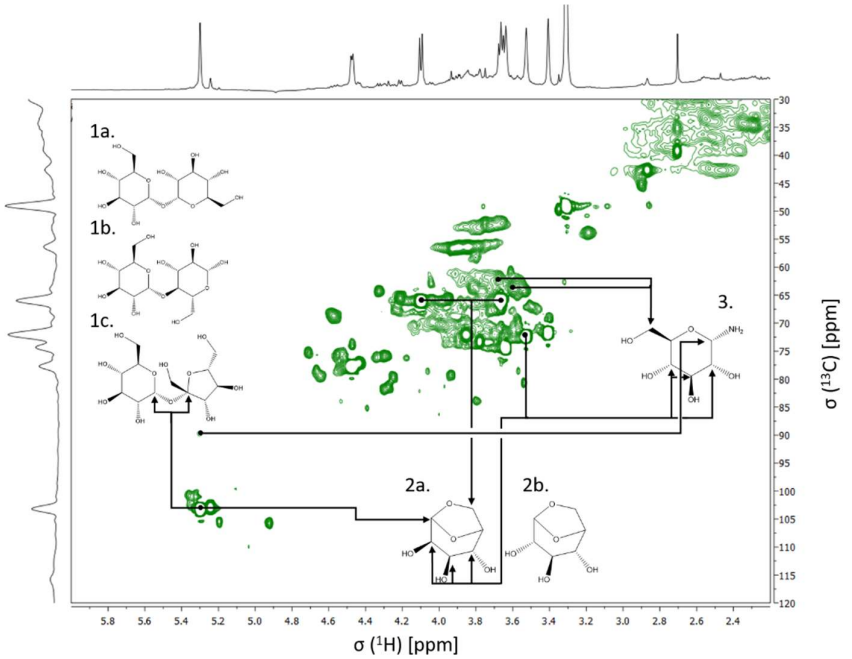

Figure 19. Expanded oxygenated aliphatic region of the ^{1}H-^{13}C HSQC spectrum of the WSOM sample collected during night time periods, with some tentative structure assignments

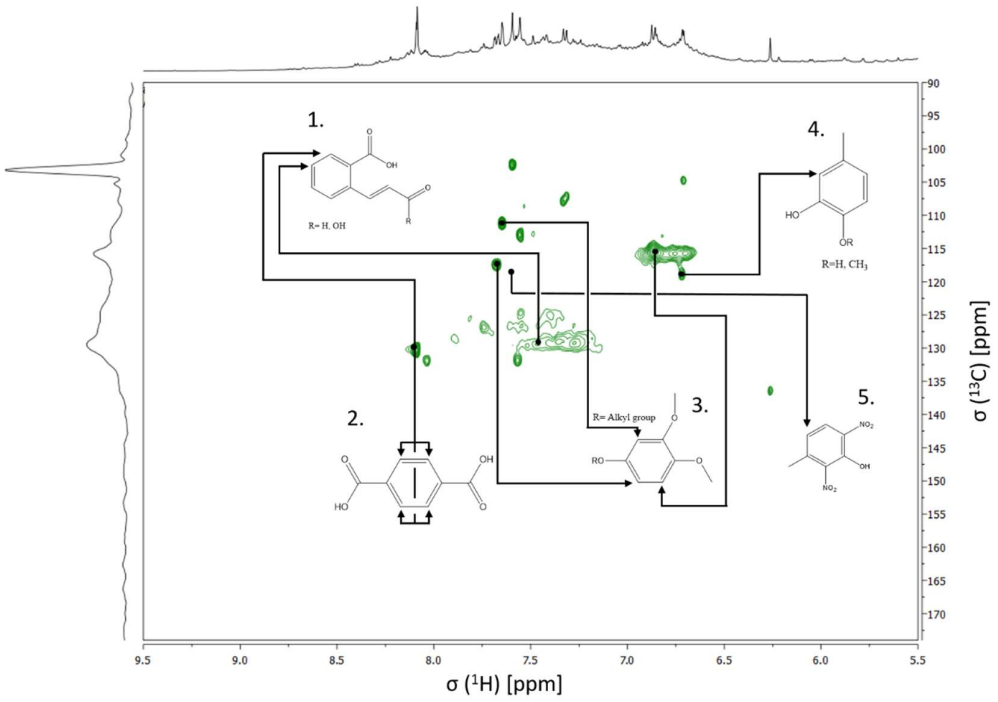

Figure 20. Expanded aromatic region of the ^{1}H-^{13}C HSQC spectrum of the WSOM sample collected during night time periods, with some tentative structure assignments

The 2D NMR signal maxima in the HSQC spectra of both day and night WSOM samples (Figures 13 and 17, respectively), showed the persistent in both samples of molecular signatures characteristic of:

(i) branched oxidized polyfunctional aliphatic structures (*e.g.*, structures 1, 2, 3a, and 3b, in Figures 14 and 18), which have been recognized as first- and/or second-generation photochemical oxidation products of different gas-phase precursors (*e.g.*, alkanes, isoprene, carbonyl, aliphatic amines, epoxides, and anhydrides) emitted from both anthropogenic (*e.g.*, biomass burning, fossil fuel combustion, and meat cooking) and natural sources (*e.g.*, sea-to-air emission of marine organics, and terrestrial vegetation) (Barnes et al., 2010; Kundu et al., 2010; Liu et al., 2011; Russell et al., 2011; Schmitt-Kopplin et al., 2012);

(ii) disaccharides (such as trehalose, maltose, and sucrose - structures 1a to 1c, respectively, in Figures 15 and 19) and anhydrosugars (such as levoglucosan and mannosan - structures 2a and 2b, respectively, Figures 15 and 19). Levoglucosan, and to a minor extent mannosan, are well-established organic molecular markers of biomass-burning emissions (Duarte et al., 2008; Simoneit et al., 1999). Dimeric sugars, such as maltose

and sucrose, could conceivably be emitted as well from the combustion of cellulose and hemi-cellulose (Nolte et al., 2001). Trehalose, on the other hand, is a fungal metabolite and it has been documented as a useful tracer of soil material and associated microbiota (Simoneit et al., 2004);

(iii) amino sugar derivatives (structure 3, Figures 15 and 19), probably reflecting the contribution of fungal-derived microbial residues in resuspended soil material (Joergensen and Wichern, 2008);

(iv) cinnamic acid and/or cinnamaldehyde (structure 1, Figures 16 and 20), and terephthalic acid (structure 2, Figures 16 and 20), possibly formed during the oxidation of aromatic hydrocarbons from urban traffic emissions (Chalbot et al., 2014; Hallquist et al., 2009; Lee et al., 2014; Matos et al., 2017)

The main differences between the two WSOM samples were verified within the aromatic region (Figures 16 and 20). The WSOM sample collected during night are enriched in highly substituted aromatic rings, where the presence of neutral (aliphatic carbon), NO_2, and/or oxygen-containing (namely, OCH_3, O-R, where R = H or alkyl group) substituents appear to be dominants. Structures 3 to 5 in Figure 20 represents some of the key aromatic substructures that are likely to be present in the night WSOM sample. Based on the 2D NMR assignments, it is clear that these aromatic structures are consistent with residues commonly found in lignin. These 2D NMR resonances have been also detected in the aromatic region of 2D NMR spectra of WSOM from rural and urban aerosol samples dominated by biomass burning (Duarte et al., 2008; Matos et al., 2017). Their presence in the night WSOM sample is plausibly explained by the emission of particulates from biomass burning for house heating, and confirms the importance of this source into the chemical composition of urban organic aerosols. Once in the atmosphere, these structures can also undergo photooxidation, originating highly oxidized SOA species. Iinuma and co-workers provided evidence that *m*-cresol, which is emitted from biomass burning at significant levels, is a precursor of methyl-nitrocatechols (similar to structure 5 in Figure 20). These SOA compounds originate from the photo-oxidation of *m*-cresol in the presence of NO_x (Iinuma et al., 2010).

3.3 Biological activity of WSOM

We started by addressing the impact of different concentrations of WSOM on the viability of Raw 264.7 macrophages. As can be seen in Figure 21, in the range of concentrations studied, none caused a significant decrease in cell viability.

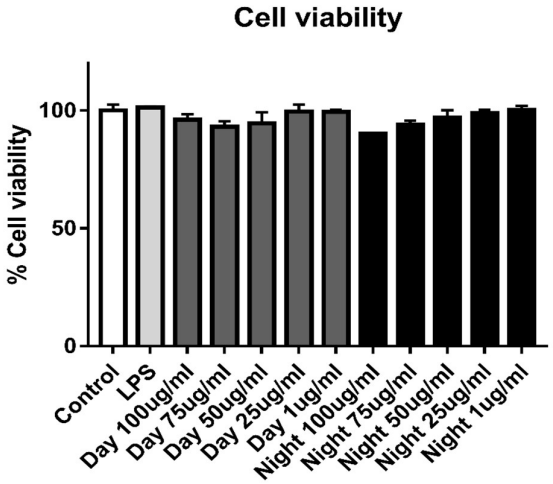

Figure 21. WSOM extracts do not significantly affect Raw 264.7 macrophages viability. Cells were exposed to different concentrations of WSOM during 24h and then viability assessed by the rezasurin assay. Data is presented as percentage of control (non-treated cells/medium) and represent the mean ± SD from at least 3 independent experiments. * significantly different (one-way ANOVA $p<0.05$) when compared to control

Simultaneously, the effects of the day and night WSOM extracts in the NO production by macrophages was assessed within the same concentration range used in viability assays (Figure 22). As can be seen neither day nor night extracts strongly induce NO production. However, we observed a small increase in some of the tested concentrations of WSOM extracts, which is also supported by the findings of Jalava and co-workers, in which they saw a small increase when using water-soluble fraction of $PM_{2.5}$ (Jalava et al., 2008). Additionally, we also observed a different tendency in the two samples. While the day extract causes a concentration dependent increase in NO production, night extract has an opposite behavior. This indicates that the later may contain compounds that induce NO production but also chemicals that counteract this effect. For the higher concentrations tested, the inhibitory effects overwhelm the induction. This behavior, observed in the night sample, does not seem to happen in the samples studied by Jalava and co-workers, which can be due to a dilution effect (caused by a continued sampling period, combining both day and night

particles) on the compounds causing these effects or due to different chemical composition of the studied samples.

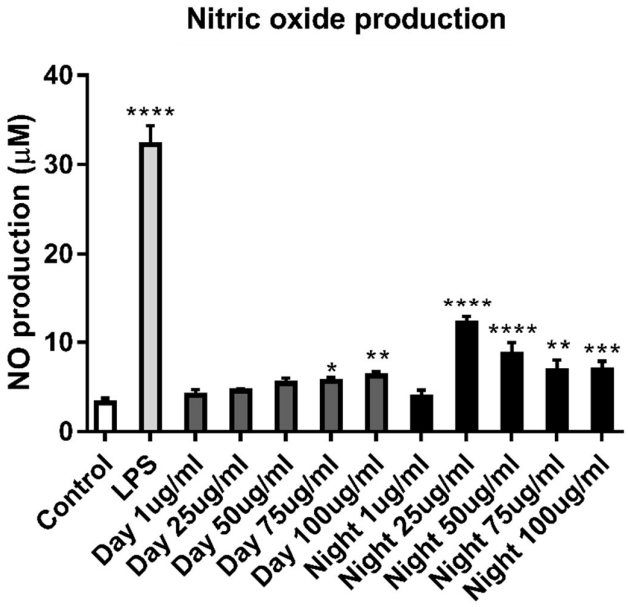

Figure 22. WSOM extracts induced NO production on raw 264.7 macrophages. Cells were exposed to different concentrations of WSOM and then their NO production was assessed by Griess assay. Data is presented as concentration of NO and represent mean ± SD from at least 3 independent experiments Multiple group comparisons (C vs conditions) was performed by one-way ANOVA analysis,with a Dunnet´s post test. Significance levels are as follows: *P<0.05, **P<0.01, ***P<0.001,and ****P<0.0001.

With these two sets of results, we decided to perform further experiences using 25µg per mL and 75µg per mL of extracts to maximize the number of assays to be performed with the available quantity of sample.

Aiming at verifying the effects of the WSOM on the macrophage transcription of several detoxifying or inflammatory molecules, we established 6 groups that were incubated for 4 hours: (1) control group – no extract was added; (2) LPS group – 1µg/ml of LPS was added; (3) Day 25 – day WSOM extract at a concentration of 25µg/mL; (4) Day 75 – day WSOM extract at 75µg/mL; (5) Night 25 – night WSOM extract at 25µg/mL; and (6) Night 75 – night WSOM extract at 75µg/mL. According to the obtained data (Figure 23), both extracts increased the transcription of *Il1b*, *Il6* and *Nos2*, although with different concentration-related effects. While for day extracts the increase in concentration is followed

by an increase in the transcription of referred genes, the opposite occurs for night extracts. Given that *Nos2* transcription is reduced by higher concentrations of night extracts this could explain the observed lower production of NO induced by these concentrations. Overall, the increase in the transcription of these genes, suggests that the studied extracts have a moderate pro-inflammatory effect. In previous studies, it has been reported a pro-inflammatory response of Raw264.7 macrophages in response to $PM_{2.5}$ (Bekki et al., 2016; Jalava et al., 2015). Particularly, Bekki and co-workers observed an increase in the transcription of *Il1b*, however they didn't observe a dose dependent response as seen in our data. This absence of the dose dependent response might be due, as previously mentioned, by a dilution effect or a different composition of the $PM_{2.5}$.

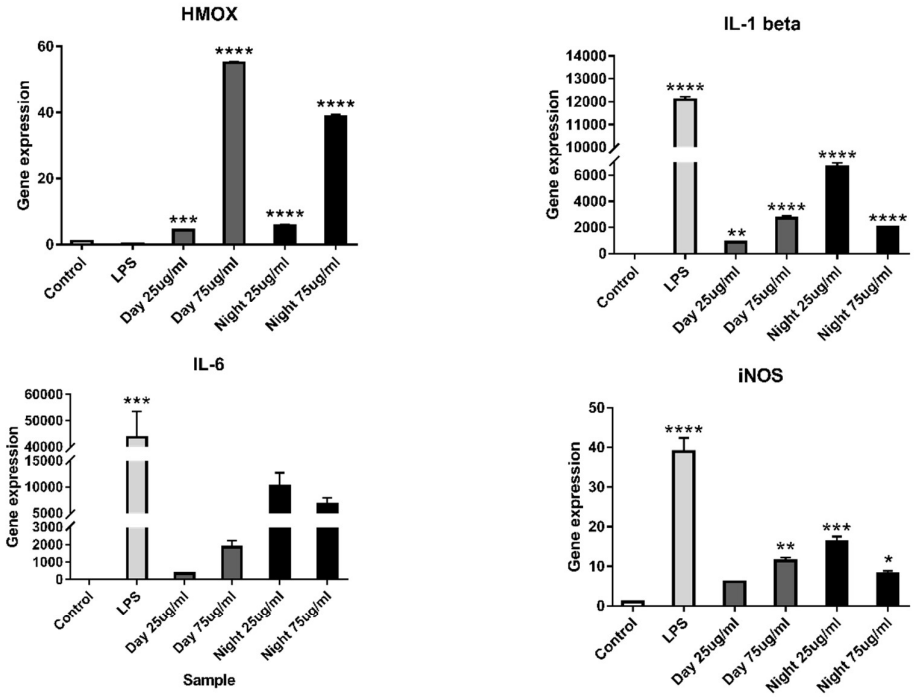

Figure 23. WSOM extracts induced an increase in the gene transcription of the studied genes on Raw 264.7 macrophages. Cells were exposed to different concentrations of WSOM extracts during 4h and then the mRNA was extracted and the gene transcription was assessed by q-PCR. Data is presented as gene expression and represent the mean ± SD from at least 2 independent experiments. Multiple group comparisons (C vs conditions) was performed by one-way ANOVA analysis,with a Dunnet´s post test. Significance levels are as follows: *P<0.05, **P<0.01, ***P<0.001,and ****P<0.0001.

Regarding *Hmox* gene, it was significantly induced by both WSOM extracts in a concentration-dependent way. *Hmox* is a detoxifying enzyme that is expressed in response to oxidative and electrophilic stresses as the result of the activation of the Keap/nrf2

signaling pathway (Kobayashi et al., 2006). Therefore, the observed increase may indicate that extracts contain compounds who cause electrophilic stress such, as the aromatic substructure 4 (in Figure 20, section 3.2) identified in the night aerosol WSOM sample. The increase in the gene expression of *Hmox* has already been described in the literature, and it was associated with the exposure to the levels of PAHs present in PM (fine and coarse) (Bachoual et al., 2007; Bekki et al., 2016; He et al., 2016), which supports the data obtained in the present study.

Next, we addressed whether WSOM extracts induce or inhibit macrophage ROS production. For this end, macrophages were incubated with different concentrations of day or night extracts or with extracts and LPS (a TLR4 agonist that will activate macrophages and induce oxidative stress). Figure 24 is a composition of 6 microscope fields representing the main observations. The results indicate that even in the higher concentrations used, extracts do not induce the production of ROS, as opposed to what is described in the literature in studies with atmospheric PM (Jalava et al., 2012; Uski et al., 2015). These discrepancies may be explained by the different material used since the majority of studies employ the whole particles, while we focused just on their water-soluble carbon fraction. Also, the observed oxidative stress on these studies might be the result of the physical interactions of the particles themselves or their content on metal ions. Surprisingly, both night and day extracts have a high antioxidant potential, completely abolishing LPS-induced oxidative stress. This may be in part due to the observed increase in the *Hmox* gene expression in cells exposed to extracts.

Moreover, we also tested if the extracts had a direct ROS scavenging activity using the *in chemico* DPPH assay. As can be seen in figure 25 both extract present a considerable ROS scavenging activity, contributing also this to striking anti-oxidant activity that we observed in cellular assays. This inhibitory effect on the capacity of macrophages to produce ROS is paradoxal: it may be beneficial given that it limits an inflammatory reaction, however, it can compromise the efficacy of macrophages to destroy harmful microorganisms during an infection by limiting the oxidative burst.

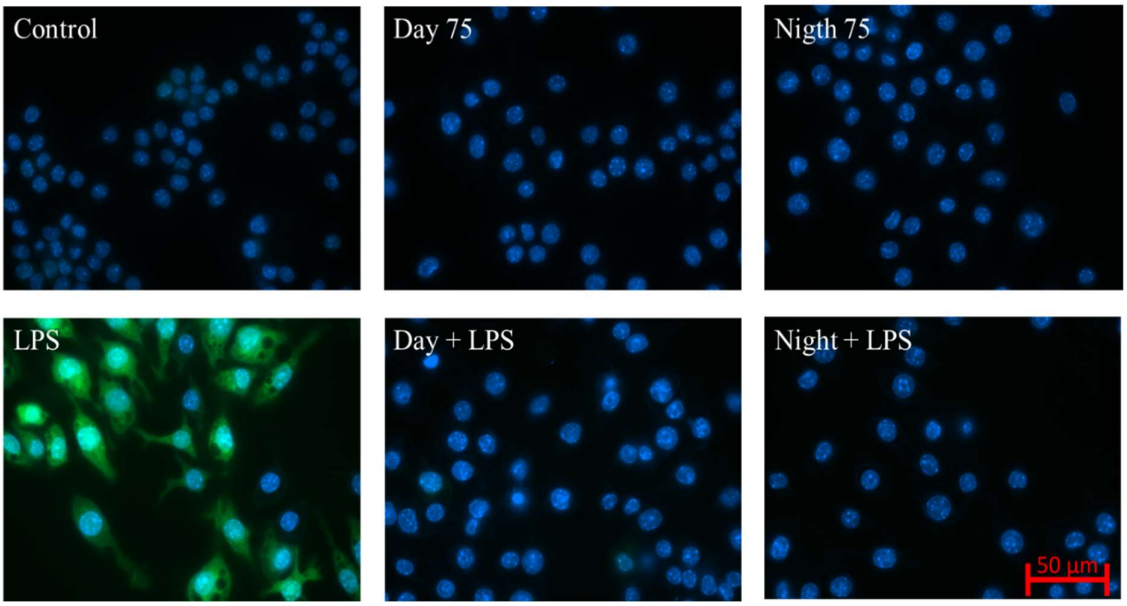

Figure 24. WSOM extracts do not induce ROS production on Raw 264.7 macrophages and abolish the LPS-induced oxidative stress. Cells were exposed to a set of different conditions and the ROS production was assessed by an *in vitro* antioxidant activity assay. Hoechst – blue (cell nucleus); H_2DCFDA – green (ROS); magnification of 63x

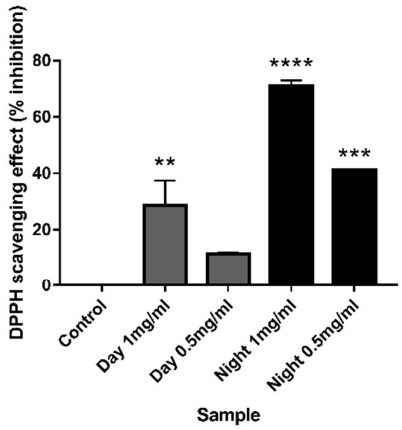

Figure 25. WSOM extracts have antioxidant activity. The antioxidant activity was assessed *in chemico* with the DPPH antioxidant activity assay. Multiple group comparisons (C vs conditions) was performed by one-way ANOVA analysis,with a Dunnet´s post test. Significance levels are as follows: *P<0.05, **P<0.01, ***P<0.001 and ****P<0.0001.

In order to verify if the WSOM extracts also caused an alteration in the macrophage capacity to produce NO, we exposed cells to the extracts and then activate them with LPS. As shown in Figure 26, both WSOM extracts (day and night) at 75µg/mL significantly inhibit LPS-induced NO production. According to our results, this effect was not due to a

direct NO scavenging activity of the extracts (Figure 27). Once again, these results show that the exposure to these aerosol components may limit macrophage oxidative burst and by inherence, their capacity to destroy invading pathogens.

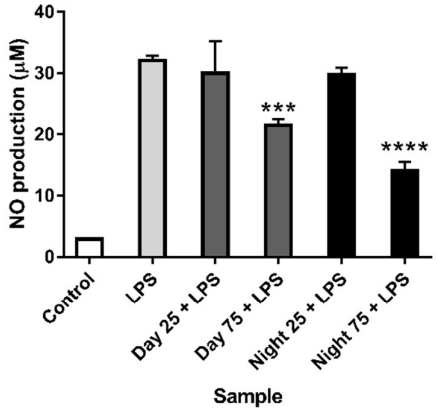

Figure 26. WSOM extracts caused a decrease in the LPS-induced NO production of raw 264.7 macrophages at higher concentrations. Cells were treated with different concentrations of WSOM extracts and then stimulated with LPS, the NO production was then assed via a Griess assay. Data is presented as concentration of NO and represent the mean ± SD from at least 3 independent experiments. Multiple group comparisons (LPS vs conditions) was performed by one-way ANOVA analysis,with a Dunnet´s post test. Significance levels are as follows: *P<0.05, **P<0.01, ***P<0.001,and ****P<0.0001.

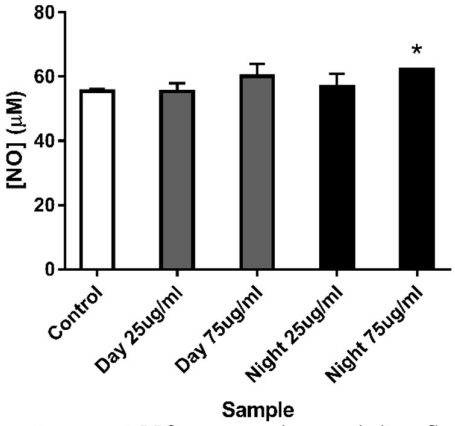

Figure 27. WSOM do not present NO scavenging activity. Scavenging activity of WSOC was assed via the SNAP assay. Data is presented as percentage of control (non-treated cells/medium) and represent the mean ± SD from at least 3 independent experiments. Multiple group comparisons (C vs conditions) was performed by one-way ANOVA analysis,with a Dunnet´s post test. Significance levels are as follows: *P<0.05.

Taking into account the obtained results, we decided to explore the potential anti-inflammatory activity of extracts. To accomplish this, macrophages were treated with extracts during 24h, exposed to LPS during additional 4h and then the transcription of several genes analyzed by qPCR. As it can be seen in Figure 28, *Hmox* gene transcription is barely affected by LPS, while it is strongly upregulated by the pretreatment with WSOM extracts, which helps to explain how extracts prevent LPS-induced oxidative stress. For *Il1b*, *Il6* and *Nos2* inflammatory genes, we found that exposure to the higher concentration of extracts (75 µg/ml) significantly decrease their LPS-induced transcription. The decrease in *Nos2* transcription can explain the decrease observed in the NO production assay (Figure 26). These results reinforce the idea that WSOM extracts may hinder the capacity of macrophages to effectively trigger an inflammatory response.

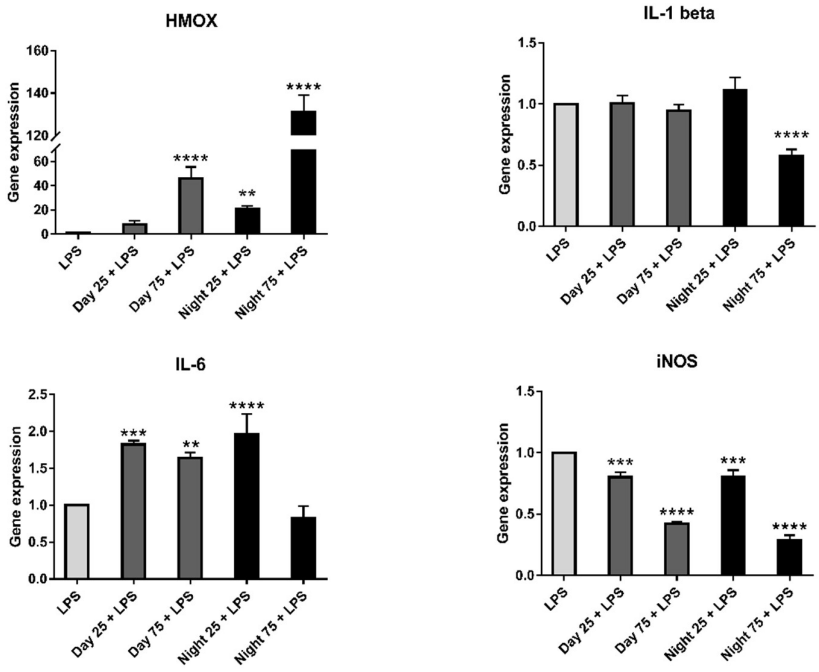

Figure 28. WSOM extracts induced alterations in the LPS-induced gene transcription of the studied genes on Raw 264.7 macrophages. Cells were exposed to different concentrations of WSOM extracts and then stimulated with LPS, then the mRNA was extracted and the gene transcription was assessed by q-PCR. Data is presented as gene expression and represent the mean ± SD from at least 3 independent experiments. Multiple group comparisons (LPS vs conditions) was performed by one-way ANOVA analysis,with a Dunnet´s post test. Significance levels are as follows: *P<0.05, **P<0.01, ***P<0.001 and ****P<0.0001.

As the transcription of inflammatory genes is the result of the activation of transcription factors such as NF-kB, we decide to assess if the inhibitory effects observed with WSOM extracts result from their inhibition of the translocation of the NF-kB to the nucleus. For this we exposed macrophages to extracts during 24h and then to LPS during additional 30 min. In some experiments, cells were just exposed to extracts. As seen in Figure 29, exposure to WSOM do not prevent the LPS-induced translocation of NF-kB (green) to the nucleus (blue). This means that the observed inhibitory effects over LPS activation are not the result of interference with the NF-kB pathway. We hypothesize that WSOM could modulate other relevant signaling pathways such as p38 and JNK MAPKs or AP1.

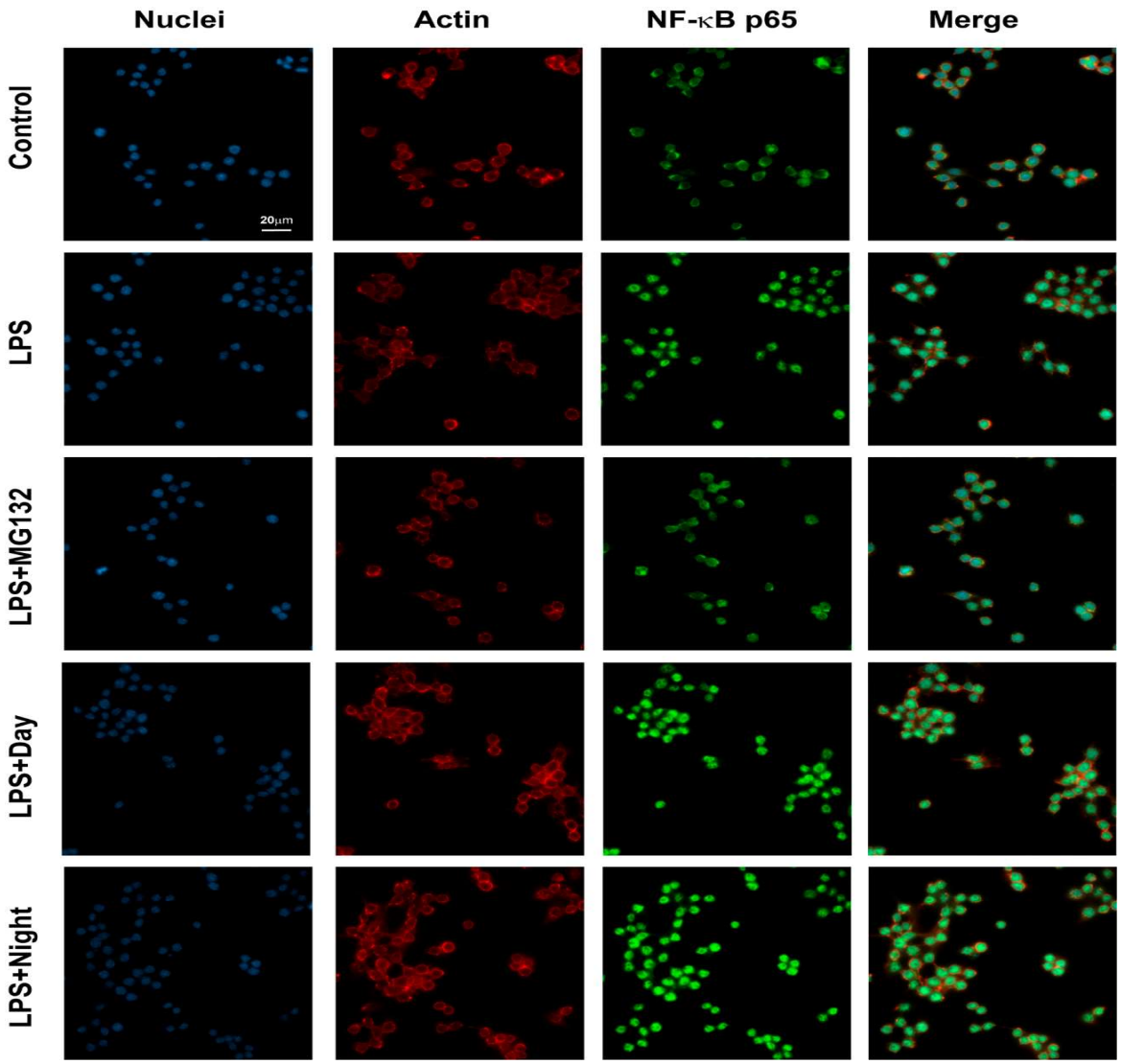

Figure 29. WSOM exposure do not prevent the LPS-induced translocation of NF-kB to the nucleus on Raw 264.7 macrophages. Cells were exposed to the WSOM extracts during 24h and then stimulated with LPS for an additional 30 min. NF-kB translocation was assessed by an immunocytochemical assay. Alexa Fluor 555 - red; Alexa Fluor 488 - green; DAPI - blue magnification of 63x

Given that all experiments were performed with acute high WSOM doses, we decided to analyze the effects of chronic exposure by culturing cells during three weeks with physiological relevant WSOM doses (*i.e.* considering the average human air intake per hour, and the atmospheric concentrations during day and night, and then administrating these quantities of WSOM extracts in day-night cycles). At the end of the three weeks, the RNA was extracted from these macrophages in order to assess the alterations induced in the transcription of studied genes. We also analyzed how these cells respond to a subsequent

exposure to an inflammatory stimulus such as LPS. The real-time q-PCR was performed in cells in 4 different conditions: control – cells incubated during the three-week cycle without WSOM extracts; LPS – equal to control but with an added stimulus of LPS; ATM – cells incubated during three weeks in a day-night cycles administration of the two WSOM extracts; ATM + LPS – cells incubated during three weeks in a day-night cycles administration of the two WSOM extracts stimulated with LPS. The results of the real-time qPCR of these cells are shown on Figure 30. The data suggest that cells exposed to WSOM present a slight increase in the transcription of *Il1b* and *Il6* by approximately 19-fold and 80-fold, respectively. However, treatment with extracts strongly impairs LPS-induced transcription of these pro-inflammatory cytokines. This suggest that prolonged exposure to these compounds leads to a diminished pro-inflammatory response in case of a new stimulus (*e.g.* microorganisms), which can translate into a least effective response against an infection.

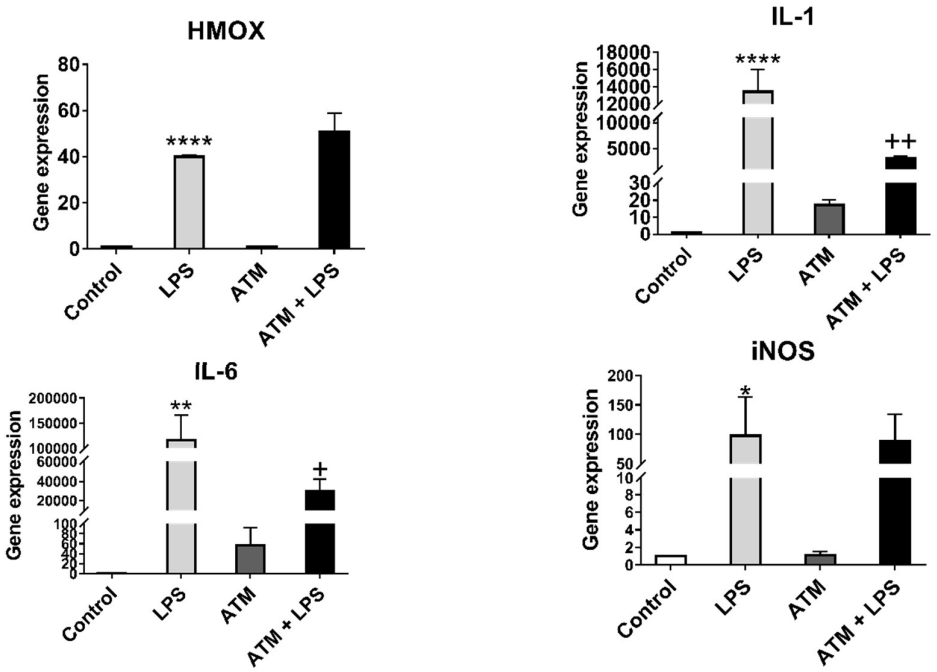

Figure 30 Prolonged exposure to physiologically relevant quantities of WSOM extracts induced alterations in the gene transcription and the LPS-induced gene transcription of the studied genes on Raw 264.7 macrophages. Cells were exposed for 3 weeks to physiologically relevant quantities of WSOM extracts, then the mRNA was extracted and the gene transcription was assessed by q-PCR. Data is presented as gene expression and represent the mean ± SD from at least 3 independent experiments. Multiple group comparisons (control vs conditions) was performed by one-way ANOVA analysis,with a Dunnet´s post test. Significance levels are as follows: *P<0.05, **P<0.01, ***P<.001,and ****P<0.0001. +significantly different (t test p<0.05) when compared to LPS; ++significantly different (t test p<0.01) when compared to LPS.

Chapter 4

Conclusions

In this work, WSOM fractions from urban $PM_{2.5}$ samples were collected during day and night periods in the autumn season of 2016, being further quantified and characterized by means of UV-Vis, EEM fluorescence, and 1D and 2D NMR spectroscopies. It was possible to verify that the highest $PM_{2.5}$ and WSOC atmospheric concentrations were verified during the night time sampling period. Moreover, the structural characterization of the WSOM samples showed that the day sample has a higher percentage of aliphatic structures, whereas the night sample was characterized by higher percentages of oxygenated and aromatic moieties. Using 2D NMR techniques, it was possible to identify the most important substructures present in both night and day WSOM samples. In particular, the night WSOM sample shows a prevalence of aromatic structures whose features are consistent with residues commonly found in lignin-derived structures. Their presence in the night WSOM sample is plausibly explained by the emission of particulates from wood burning for house heating, and confirms the importance of this source into the chemical composition of urban organic aerosols.

The biological activity of both day and night WSOM samples was also evaluated in raw264.7 macrophages, following two different types of exposure: i) acute response study and ii) a more chronic study. In the acute exposure studies, it was possible to see that these compounds induced an increase in the transcription of *Il1b*, *Il6*, *Nos2* and *Hmox*, indicating that at high doses they stimulated a moderate pro-inflammatory profile in macrophages. We also found that WSOM extracts do not induced ROS production, instead, these WSOM extracts can effectively inhibit LPS-induced oxidative stress. This antioxidant effect is in part due to intrinsic ROS scavenging activity and by the capacity of extracts to strongly induce the transcription of *Hmox* detoxifying gene. Surprisingly, pre-treatment of cells with WSOM extracts limit their capacity to produce inflammatory mediators IL-1b, IL-6 and iNOS in a subsequent exposure to LPS. These results suggest that the capacity of macrophages to manage invading microorganisms and limit infections may be compromised by exposure to $PM_{2.5,}$ namely to their WSOM fraction.

In order to assess the effect of prolonged exposure to the WSOM extracts in a scenario resembling a real-life situation, cells were stimulated in day-night cycles with physiological quantities of WSOM extracts (based on the average volume of air inspired by humans). According to obtained data, it was possible to see that a prolonged exposure to very small

concentration of these compounds cause a decrease in the capacity of macrophages to respond to a subsequent inflammatory stimulus.

Overall, our results indicate that exposure to WSOM fraction of $PM_{2.5}$ may compromise the capacity of macrophages to mount an effective inflammatory response, required to manage harmful pathogens. Therefore, continuous and prolonged exposure to these compounds could result in increased susceptibility to respiratory infections.

References

Anderson, C., Dibb, J.E., Griffin, R.J., Bergin, M.H., 2008. Simultaneous measurements of particulate and gas-phase water-soluble organic carbon concentrations at remote and urban-influenced locations. Geophys. Res. Lett. 35.

Atkinson, R., 2000. Atmospheric chemistry of VOCs and NOx. Atmos. Environ. 34, 2063–2101.

Bachoual, R., Boczkowski, J., Goven, D., Amara, N., Tabet, L., On, D., Leçon-Malas, V., Aubier, M., Lanone, S., 2007. Biological Effects of Particles from the Paris Subway System. Chem. Res. Toxicol. 20, 1426–1433.

Barnes, I., Solignac, G., Mellouki, A., Becker, K.H., 2010. Aspects of the Atmospheric Chemistry of Amides. ChemPhysChem 11, 3844–3857.

Bauer, R.N., Diaz-Sanchez, D., Jaspers, I., 2012. Effects of air pollutants on innate immunity: The role of Toll-like receptors and nucleotide-binding oligomerization domain–like receptors. J. Allergy Clin. Immunol. 129, 14–24.

Bekki, K., Ito, T., Yoshida, Y., He, C., Arashidani, K., He, M., Sun, G., Zeng, Y., Sone, H., Kunugita, N., Ichinose, T., 2016. PM 2.5 collected in China causes inflammatory and oxidative stress responses in macrophages through the multiple pathways. Environ. Toxicol. Pharmacol. 45, 362–369.

Calvo, A.I., Alves, C., Castro, A., Pont, V., Vicente, A.M., Fraile, R., 2013. Research on aerosol sources and chemical composition: Past, current and emerging issues. Atmospheric Res. 120–121, 1–28.

Cassee, F.R., Héroux, M.-E., Gerlofs-Nijland, M.E., Kelly, F.J., 2013. Particulate matter beyond mass: recent health evidence on the role of fractions, chemical constituents and sources of emission. Inhal. Toxicol. 25, 802–812.

Chalbot, M.-C.G., Brown, J., Chitranshi, P., Gamboa da Costa, G., Pollock, E.D., Kavouras, I.G., 2014. Functional characterization of the water-soluble organic carbon of size-fractionated aerosol in the southern Mississippi Valley. Atmospheric Chem. Phys. 14, 6075–6088.

Charo, I.F., Ransohoff, R.M., 2006. The Many Roles of Chemokines and Chemokine Receptors in Inflammation. N. Engl. J. Med. 354, 610–621.

Chauhan, V., Breznan, D., Goegan, P., Nadeau, D., Karthikeyan, S., Brook, J.R., Vincent, R., 2004. Effects of ambient air particles on nitric oxide production in macrophage cell lines. Cell Biol. Toxicol. 20, 221–239.

Chen, Q., Ikemori, F., Mochida, M., 2016a. Light Absorption and Excitation–Emission Fluorescence of Urban Organic Aerosol Components and Their Relationship to Chemical Structure. Environ. Sci. Technol. 50, 10859–10868.

Chen, Q., Miyazaki, Y., Kawamura, K., Matsumoto, K., Coburn, S., Volkamer, R., Iwamoto, Y., Kagami, S., Deng, Y., Ogawa, S., Ramasamy, S., Kato, S., Ida, A., Kajii, Y., Mochida, M., 2016b. Characterization of Chromophoric Water-Soluble Organic Matter in Urban, Forest, and Marine Aerosols by HR-ToF-AMS Analysis and Excitation–Emission Matrix Spectroscopy. Environ. Sci. Technol. 50, 10351–10360.

Cirino, G., Distrutti, E., Wallace, J., 2006. Nitric Oxide and Inflammation. Inflamm. Allergy-Drug Targets 5, 115–119.

Daher, N., Ruprecht, A., Invernizzi, G., De Marco, C., Miller-Schulze, J., Heo, J.B., Shafer, M.M., Shelton, B.R., Schauer, J.J., Sioutas, C., 2012. Characterization, sources and redox activity of fine and coarse particulate matter in Milan, Italy. Atmos. Environ. 49, 130–141.

Danielsen, P.H., Loft, S., Jacobsen, N.R., Jensen, K.A., Autrup, H., Ravanat, J.-L., Wallin, H., Moller, P., 2010. Oxidative Stress, Inflammation, and DNA Damage in Rats after

Intratracheal Instillation or Oral Exposure to Ambient Air and Wood Smoke Particulate Matter. Toxicol. Sci. 118, 574–585.
Decesari, S., Facchini, M.C., Fuzzi, S., Tagliavini, E., 2000. Characterization of water-soluble organic compounds in atmospheric aerosol: A new approach. J. Geophys. Res. Atmospheres 105, 1481–1489.
Dinar, E., Abo Riziq, A., Spindler, C., Erlick, C., Kiss, G., Rudich, Y., 2008. The complex refractive index of atmospheric and model humic-like substances (HULIS) retrieved by a cavity ring down aerosol spectrometer (CRD-AS). Faraday Discuss 137, 279–295.
Dinar, E., Taraniuk, I., Graber, E.R., Katsman, S., Moise, T., Anttila, T., Mentel, T.F., Rudich, Y., 2006. Cloud Condensation Nuclei properties of model and atmospheric HULIS. Atmospheric Chem. Phys. 6, 2465–2482.
Duarte, R.M.B.O., Duarte, A.C., 2011. A critical review of advanced analytical techniques for water-soluble organic matter from atmospheric aerosols. TrAC Trends Anal. Chem. 30, 1659–1671.
Duarte, R.M.B.O., Freire, S.M.S.C., Duarte, A.C., 2015. Investigating the water-soluble organic functionality of urban aerosols using two-dimensional correlation of solid-state 13C NMR and FTIR spectral data. Atmos. Environ. 116, 245–252.
Duarte, R.M.B.O., Matos, J.T.V., Paula, A.S., Lopes, S.P., Ribeiro, S., Santos, J.F., Patinha, C., da Silva, E.F., Soares, R., Duarte, A.C., 2016. Tracing of aerosol sources in an urban environment using chemical, Sr isotope, and mineralogical characterization. Environ. Sci. Pollut. Res.
Duarte, R.M.B.O., Pio, C.A., Duarte, A.C., 2005. Spectroscopic study of the water-soluble organic matter isolated from atmospheric aerosols collected under different atmospheric conditions. Anal. Chim. Acta 530, 7–14.
Duarte, R.M.B.O., Santos, E.B.H., Pio, C.A., Duarte, A.C., 2007. Comparison of structural features of water-soluble organic matter from atmospheric aerosols with those of aquatic humic substances. Atmos. Environ. 41, 8100–8113.
Duarte, R.M.B.O., Silva, A.M.S., Duarte, A.C., 2008. Two-Dimensional NMR Studies of Water-Soluble Organic Matter in Atmospheric Aerosols. Environ. Sci. Technol. 42, 8224–8230.
Fine, P.M., Cass, G.R., Simoneit, B.R.T., 2001. Chemical Characterization of Fine Particle Emissions from Fireplace Combustion of Woods Grown in the Northeastern United States. Environ. Sci. Technol. 35, 2665–2675.
Fujii, T., Hayashi, S., Hogg, J.C., Vincent, R., Van Eeden, S.F., 2001. Particulate Matter Induces Cytokine Expression in Human Bronchial Epithelial Cells. Am. J. Respir. Cell Mol. Biol. 25, 265–271.
Gelencsér A, May B, Simpson D, Sánchez-Ochoa A, Kasper-Giebl A, Puxbaum H, Caseiro A, Pio C, Legrand M. Source apportionment of PM2.5 organic aerosol over Europe: Primary/secondary, natural/anthropogenic, and fossil/biogenic origin. J Geophys Res. 2007 Sep.
Griffith, E.C., Carpenter, B.K., Shoemaker, R.K., Vaida, V., 2013. Photochemistry of aqueous pyruvic acid. Proc. Natl. Acad. Sci. 110, 11714–11719.
Hallquist, M., Wenger, J.C., Baltensperger, U., Rudich, Y., Simpson, D., Claeys, M., Dommen, J., Donahue, N.M., George, C., Goldstein, A.H., Hamilton, J.F., Herrmann, H., Hoffmann, T., Iinuma, Y., Jang, M., Jenkin, M.E., Jimenez, J.L., Kiendler-Scharr, A., Maenhaut, W., McFiggans, G., Mentel, T.F., Monod, A., Prévôt, A.S.H., Seinfeld, J.H., Surratt, J.D., Szmigielski, R., Wildt, J., 2009. The

formation, properties and impact of secondary organic aerosol: current and emerging issues. Atmospheric Chem. Phys. 9, 5155–5236.
He, M., Ichinose, T., Yoshida, S., Shiba, F., Arashidani, K., Takano, H., Sun, G., Shibamoto, T., 2016. Differences in allergic inflammatory responses in murine lungs: comparison of PM2.5 and coarse PM collected during the hazy events in a Chinese city. Inhal. Toxicol. 28, 706–718.
Hoek, G., Krishnan, R.M., Beelen, R., Peters, A., Ostro, B., Brunekreef, B., Kaufman, J.D., 2013. Long-term air pollution exposure and cardio-respiratory mortality: a review. Environ. Health 12, 1.
Iinuma, Y., Böge, O., Gräfe, R., Herrmann, H., 2010. Methyl-Nitrocatechols: Atmospheric Tracer Compounds for Biomass Burning Secondary Organic Aerosols. Environ. Sci. Technol. 44, 8453–8459.
Jaiprakash, Singhai, A., Habib, G., Raman, R.S., Gupta, T., 2017. Chemical characterization of PM1.0 aerosol in Delhi and source apportionment using positive matrix factorization. Environ. Sci. Pollut. Res. 24, 445–462.
Jalava, P.I., Aakko-Saksa, P., Murtonen, T., Happo, M.S., Markkanen, A., Yli-Pirilä, P., Hakulinen, P., Hillamo, R., Mäki-Paakkanen, J., Salonen, R.O., 2012. Toxicological properties of emission particles from heavy duty engines powered by conventional and bio-based diesel fuels and compressed natural gas. Part. Fibre Toxicol. 9, 37.
Jalava, P.I., Happo, M.S., Huttunen, K., Sillanpää, M., Hillamo, R., Salonen, R.O., Hirvonen, M.-R., 2015. Chemical and microbial components of urban air PM cause seasonal variation of toxicological activity. Environ. Toxicol. Pharmacol. 40, 375–387.
Jalava, P.I., Salonen, R.O., Pennanen, A.S., Happo, M.S., Penttinen, P., Hälinen, A.I., Sillanpää, M., Hillamo, R., Hirvonen, M.-R., 2008. Effects of solubility of urban air fine and coarse particles on cytotoxic and inflammatory responses in RAW 264.7 macrophage cell line. Toxicol. Appl. Pharmacol. 229, 146–160.
Jang, A.-S., 2012. Particulate Air Pollutants and Respiratory Diseases, in: Haryanto, B. (Ed.), Air Pollution - A Comprehensive Perspective. InTech.
Joergensen, R., Wichern, F., 2008. Quantitative assessment of the fungal contribution to microbial tissue in soil. Soil Biol. Biochem. 40, 2977–2991.
Jurado, E., Dachs, J., Duarte, C.M., Simó, R., 2008. Atmospheric deposition of organic and black carbon to the global oceans. Atmos. Environ. 42, 7931–7939.
Kim, K.-H., Kabir, E., Kabir, S., 2015. A review on the human health impact of airborne particulate matter. Environ. Int. 74, 136–143.
Kobayashi, A., Kang, M.-I., Watai, Y., Tong, K.I., Shibata, T., Uchida, K., Yamamoto, M., 2006. Oxidative and Electrophilic Stresses Activate Nrf2 through Inhibition of Ubiquitination Activity of Keap1. Mol. Cell. Biol. 26, 221–229.
Kumar, V., Robbins, S.L., Cotran, R.S. (Eds.), 2010. Robbins and Cotran pathologic basis of disease:, 8. ed. ed. Elsevier, Saunders, Philadelphia, Pa.
Kundu, S., Kawamura, K., Andreae, T.W., Hoffer, A., Andreae, M.O., 2010. Molecular distributions of dicarboxylic acids, ketocarboxylic acids and α-dicarbonyls in biomass burning aerosols: implications for photochemical production and degradation in smoke layers. Atmospheric Chem. Phys. 10, 2209–2225.
Laroux, F.S., Pavlick, K.P., Hines, I.N., Kawachi, S., Harada, H., Bharwani, S., Hoffman, J.M., Grisham, M.B., 2001. Role of nitric oxide in inflammation. Acta Physiol. Scand. 173, 113–118.

Lee, H.J. (Julie), Aiona, P.K., Laskin, A., Laskin, J., Nizkorodov, S.A., 2014. Effect of Solar Radiation on the Optical Properties and Molecular Composition of Laboratory Proxies of Atmospheric Brown Carbon. Environ. Sci. Technol. 48, 10217–10226.

Li, N., Xia, T., Nel, A.E., 2008. The role of oxidative stress in ambient particulate matter-induced lung diseases and its implications in the toxicity of engineered nanoparticles. Free Radic. Biol. Med. 44, 1689–1699.

Li, R., Kou, X., Xie, L., Cheng, F., Geng, H., 2015. Effects of ambient PM2.5 on pathological injury, inflammation, oxidative stress, metabolic enzyme activity, and expression of c-fos and c-jun in lungs of rats. Environ. Sci. Pollut. Res. 22, 20167–20176.

Liu, S., Day, D.A., Shields, J.E., Russell, L.M., 2011. Ozone-driven daytime formation of secondary organic aerosol containing carboxylic acid groups and alkane groups. Atmospheric Chem. Phys. 11, 8321–8341.

Lopes, C.B., Abreu, S., Válega, M., Duarte, R.M.B.O., Pereira, M.E., Duarte, A.C., 2006. The Assembling and Application of an Automated Segmented Flow Analyzer for the Determination of Dissolved Organic Carbon Based on UV-Persulphate Oxidation. Anal. Lett. 39, 1979–1992.

Lopes, S.P., Matos, J.T.V., Silva, A.M.S., Duarte, A.C., Duarte, R.M.B.O., 2015. 1H NMR studies of water- and alkaline-soluble organic matter from fine urban atmospheric aerosols. Atmos. Environ. 119, 374–380.

Maksymiuk, C.S., Gayahtri, C., Gil, R.R., Donahue, N.M., 2009. Secondary organic aerosol formation from multiphase oxidation of limonene by ozone: mechanistic constraints via two-dimensional heteronuclear NMR spectroscopy. Phys. Chem. Chem. Phys. 11, 7810–7818.

Martin, T.R., 2005. Innate Immunity in the Lungs. Proc. Am. Thorac. Soc. 2, 403–411.

Matos, J.T.V., Duarte, R.M.B.O., Lopes, S.P., Silva, A.M.S., Duarte, A.C., 2017. Persistence of urban organic aerosols composition: Decoding their structural complexity and seasonal variability. Environ. Pollut. 231, 281–290.

Matos, J.T.V., Freire, S.M.S.C., Duarte, R.M.B.O., Duarte, A.C., 2015. Natural organic matter in urban aerosols: Comparison between water and alkaline soluble components using excitation–emission matrix fluorescence spectroscopy and multiway data analysis. Atmos. Environ. 102, 1–10.

Mazzeo, N. (Ed.), 2011. Organic Compounds in Airborne Particles and their Genotoxic Effects in Mexico City, in: Air Quality Monitoring, Assessment and Management. InTech.

Mazzoli-Rocha, F., Fernandes, S., Einicker-Lamas, M., Zin, W.A., 2010. Roles of oxidative stress in signaling and inflammation induced by particulate matter. Cell Biol. Toxicol. 26, 481–498.

Michael, S., Montag, M., Dott, W., 2013. Pro-inflammatory effects and oxidative stress in lung macrophages and epithelial cells induced by ambient particulate matter. Environ. Pollut. 183, 19–29.

Miller, F.J., Gardner, D.E., Graham, J.A., Lee, R.E., Wilson, W.E., Bachmann, J.D., 1979. Size Considerations for Establishing a Standard for Inhalable Particles. J. Air Pollut. Control Assoc. 29, 610–615.

Mladenov, N., Reche, I., Olmo, F.J., Lyamani, H., Alados-Arboledas, L., 2010. Relationships between spectroscopic properties of high-altitude organic aerosols and Sun photometry from ground-based remote sensing. J. Geophys. Res. 115.

Nathan, C., 2002. Points of control in inflammation. Nature 420, 846–852.

Nolte, C.G., Schauer, J.J., Cass, G.R., Simoneit, B.R.T., 2001. Highly Polar Organic Compounds Present in Wood Smoke and in the Ambient Atmosphere. Environ. Sci. Technol. 35, 1912–1919.

O'Brien, J., Wilson, I., Orton, T., Pognan, F., 2000. Investigation of the Alamar Blue (resazurin) fluorescent dye for the assessment of mammalian cell cytotoxicity. Eur. J. Biochem. 267, 5421–5426.

Øvrevik, J., Refsnes, M., Låg, M., Holme, J., Schwarze, P., 2015. Activation of Proinflammatory Responses in Cells of the Airway Mucosa by Particulate Matter: Oxidant- and Non-Oxidant-Mediated Triggering Mechanisms. Biomolecules 5, 1399–1440.

Padró, L.T., Tkacik, D., Lathem, T., Hennigan, C.J., Sullivan, A.P., Weber, R.J., Huey, L.G., Nenes, A., 2010. Investigation of cloud condensation nuclei properties and droplet growth kinetics of the water-soluble aerosol fraction in Mexico City. J. Geophys. Res. 115.

Paglione, M., Saarikoski, S., Carbone, S., Hillamo, R., Facchini, M.C., Finessi, E., Giulianelli, L., Carbone, C., Fuzzi, S., Moretti, F., Tagliavini, E., Swietlicki, E., Eriksson Stenström, K., Prévôt, A.S.H., Massoli, P., Canaragatna, M., Worsnop, D., Decesari, S., 2014. Primary and secondary biomass burning aerosols determined by proton nuclear magnetic resonance (1H-NMR) spectroscopy during the 2008 EUCAARI campaign in the Po Valley (Italy). Atmospheric Chem. Phys. 14, 5089–5110.

Pope, C.A., Burnett, R.T., Thun, M.J., Calle, E.E., Krewski, D., Ito, K., Thurston, G.D., 2002. Lung Cancer, Cardiopulmonary Mortality, and Long-term Exposure to Fine Particulate Air Pollution. JAMA 1132–1141.

Pope, C.A., Ezzati, M., Dockery, D.W., 2009. Fine-Particulate Air Pollution and Life Expectancy in the United States. N. Engl. J. Med. 376–386.

Powerpoint image bank | Servier [WWW Document], n.d. URL http://www.servier.com/Powerpoint-image-bank (accessed 11.16.16).

Putaud, J.-P., Van Dingenen, R., Alastuey, A., Bauer, H., Birmili, W., Cyrys, J., Flentje, H., Fuzzi, S., Gehrig, R., Hansson, H.-C., 2010. A European aerosol phenomenology–3: Physical and chemical characteristics of particulate matter from 60 rural, urban, and kerbside sites across Europe. Atmos. Environ. 44, 1308–1320.

Ricciotti, E., FitzGerald, G.A., 2011. Prostaglandins and Inflammation. Arterioscler. Thromb. Vasc. Biol. 31, 986–1000.

Risom, L., Møller, P., Loft, S., 2005. Oxidative stress-induced DNA damage by particulate air pollution. Mutat. Res. Mol. Mech. Mutagen. 592, 119–137.

Rolph, G., Stein, A., Stunder, B., 2017. Real-time Environmental Applications and Display sYstem: READY. Environ. Model. Softw. 95, 210–228.

Russell, L.M., Bahadur, R., Ziemann, P.J., 2011. Identifying organic aerosol sources by comparing functional group composition in chamber and atmospheric particles. Proc. Natl. Acad. Sci. 108, 3516–3521.

Saffari, A., Daher, N., Shafer, M.M., Schauer, J.J., Sioutas, C., 2014. Global Perspective on the Oxidative Potential of Airborne Particulate Matter: A Synthesis of Research Findings. Environ. Sci. Technol. 48, 7576–7583.

Sallusto, F., Mackay, C.R., 2004. Chemoattractants and their receptors in homeostasis and inflammation. Curr. Opin. Immunol. 16, 724–731.

Salvemini, D., Doyle, T.M., Cuzzocrea, S., 2006. Superoxide, peroxynitrite and oxidative/nitrative stress in inflammation. Biochem. Soc. Trans. 34, 965–970.

Samara, C., Voutsa, D., 2005. Size distribution of airborne particulate matter and associated heavy metals in the roadside environment. Chemosphere 59, 1197–1206.
Schauer, J.J., Rogge, W.F., Hildemann, L.M., Mazurek, M.A., Cass, G.R., 1996. Source apportionment of airborne particulate matter using organic compounds as tracers. Atmos. Environ. 30, 3837–3855.
Schmitt-Kopplin, P., Gelencsér, A., Dabek-Zlotorzynska, E., Kiss, G., Hertkorn, N., Harir, M., Hong, Y., Gebefügi, I., 2010. Analysis of the Unresolved Organic Fraction in Atmospheric Aerosols with Ultrahigh-Resolution Mass Spectrometry and Nuclear Magnetic Resonance Spectroscopy: Organosulfates As Photochemical Smog Constituents †. Anal. Chem. 82, 8017–8026.
Schmitt-Kopplin, P., Liger-Belair, G., Koch, B.P., Flerus, R., Kattner, G., Harir, M., Kanawati, B., Lucio, M., Tziotis, D., Hertkorn, N., Gebefügi, I., 2012. Dissolved organic matter in sea spray: a transfer study from marine surface water to aerosols. Biogeosciences 9, 1571–1582.
Schwarze, P.E., Ovrevik, J., Lag, M., Refsnes, M., Nafstad, P., Hetland, R.B., Dybing, E., 2006. Particulate matter properties and health effects: consistency of epidemiological and toxicological studies. Hum. Exp. Toxicol. 25, 559–579.
Seinfeld JH, Pandis SN. Atmospheric chemistry and physics: from air pollution to climate change. 2nd ed. Hoboken, N.J: J. Wiley; 2006.
Senesi, N., Xing, B., Huang, P.M. (Eds.), 2009. Natural Organic Matter in Atmospheric Particles, in: Biophysico-Chemical Processes Involving Natural Nonliving Organic Matter in Environmental Systems, Wiley-IUPAC Series in Biophysico-Chemical Processes in Environmental Systems. Wiley, Hoboken, N.J, pp. 451–486.
Serhan, C.N. (Ed.), 2010. Fundamentals of inflammation. Cambridge Univ. Press, Cambridge.
Serhan, C.N., Chiang, N., Van Dyke, T.E., 2008. Resolving inflammation: dual anti-inflammatory and pro-resolution lipid mediators. Nat. Rev. Immunol. 8, 349–361.
Serhan, C.N., Savill, J., 2005. Resolution of inflammation: the beginning programs the end. Nat. Immunol. 6, 1191–1197.
Simoneit, B.R.T., Elias, V.O., Kobayashi, M., Kawamura, K., Rushdi, A.I., Medeiros, P.M., Rogge, W.F., Didyk, B.M., 2004. SugarsDominant Water-Soluble Organic Compounds in Soils and Characterization as Tracers in Atmospheric Particulate Matter. Environ. Sci. Technol. 38, 5939–5949.
Simoneit, B.R.T., Schauer, J.J., Nolte, C.G., Oros, D.R., Elias, V.O., Fraser, M.P., Rogge, W.F., Cass, G.R., 1999. Levoglucosan, a tracer for cellulose in biomass burning and atmospheric particles. Atmos. Environ. 33, 173–182.
Stafforini, D.M., McIntyre, T.M., Zimmerman, G.A., Prescott, S.M., 2003. Platelet-Activating Factor, a Pleiotrophic Mediator of Physiological and Pathological Processes. Crit. Rev. Clin. Lab. Sci. 40, 643–672.
Stein, A.F., Draxler, R.R., Rolph, G.D., Stunder, B.J.B., Cohen, M.D., Ngan, F., 2015. NOAA's HYSPLIT Atmospheric Transport and Dispersion Modeling System. Bull. Am. Meteorol. Soc. 96, 2059–2077.
Stenfors, N., Nordenhall, C., Salvi, S.S., Mudway, I., Soderberg, M., Blomberg, A., Helleday, R., Levin, J.-O., Holgate, S.T., Kelly, F.J., Frew, A.J., Sandstrom, T., 2004. Different airway inflammatory responses in asthmatic and healthy humans exposed to diesel. Eur. Respir. J. 23, 82–86.
Tagliavini, E., Moretti, F., Decesari, S., Facchini, M.C., Fuzzi, S., Maenhaut, W., 2006. Functional group analysis by H NMR/chemical derivatization for the

characterization of organic aerosol from the SMOCC field campaign. Atmospheric Chem. Phys. 6, 1003–1019.
Totlandsdal, A.I., Cassee, F.R., Schwarze, P., Refsnes, M., L\a ag, M., 2010. Diesel exhaust particles induce CYP1A1 and pro-inflammatory responses via differential pathways in human bronchial epithelial cells. Part. Fibre Toxicol. 7, 1.
Tracey, K.J., 2002. The inflammatory reflex. Nature 420, 853–859.
Uski, O., Jalava, P.I., Happo, M.S., Torvela, T., Leskinen, J., Mäki-Paakkanen, J., Tissari, J., Sippula, O., Lamberg, H., Jokiniemi, J., Hirvonen, M.-R., 2015. Effect of fuel zinc content on toxicological responses of particulate matter from pellet combustion in vitro. Sci. Total Environ. 511, 331–340.

Annexes

A1. Meteorological conditions during the sampling campaigns

Table A1. Meteorological data collected during the sampling period.

Sampling period	Range and median values of Air temperature (ºC)	Precipitation[(a)] (mm H_2O)	Maximum wind velocity (m s^{-1})	Origin of air masses[(b)]
Day – **week 1**	20 - 12; 16	0.0	4.5	Continental/maritime
Night – **week 1**	18 - 10; 13	1.3	3.7	Continental/maritime
Day – **week 2**	16 - 8.2; 13	2.3	3.6	Continental/maritime
Night – **week 2**	13 - 4.1; 9.7	1.5	1.4	Continental/maritime

(a)Total precipitation accumulated during the sampling period

(b) Origin of air masses during each season, based on air mass back trajectories assessed by means of the HYbrid Single Particle Lagrangian Integrated Trajectory (HYSPLIT) model, using the Global Data Assimilation System (GDAS)meteorological database, and accessed via National Oceanic and Atmospheric Administration (NOAA) Air Resources Laboratory READY website (Rolph et al., 2017; Stein et al., 2015)

A2. UV-vis spectroscopy of the WSOM samples

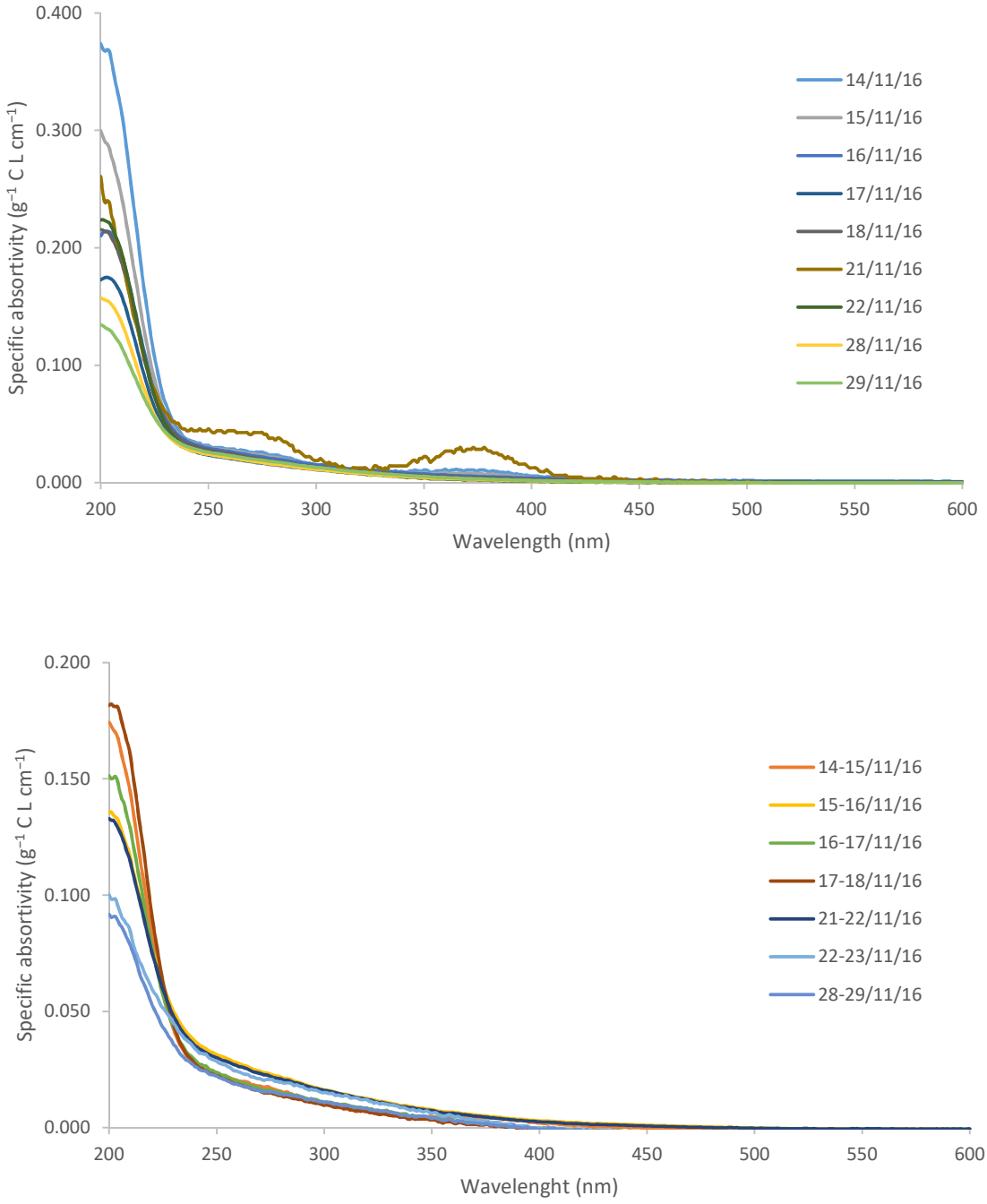

Figure A1. UV-visible spectra of the aerosol WSOM samples collected in different time periods: day (up) and night (down)

A3. EEM fluorescence spectroscopy of fine urban aerosol WSOM samples

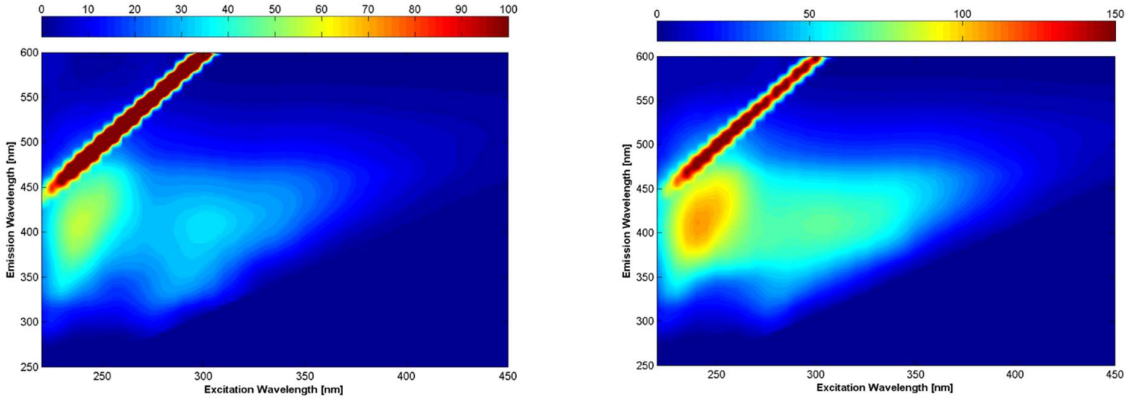

Figure A2. EEM fluorescence spectra of the aerosol WSOM samples collected in different time periods: day (left, 14/11/16) and night (right, 14/11/16 to 15/11/16)

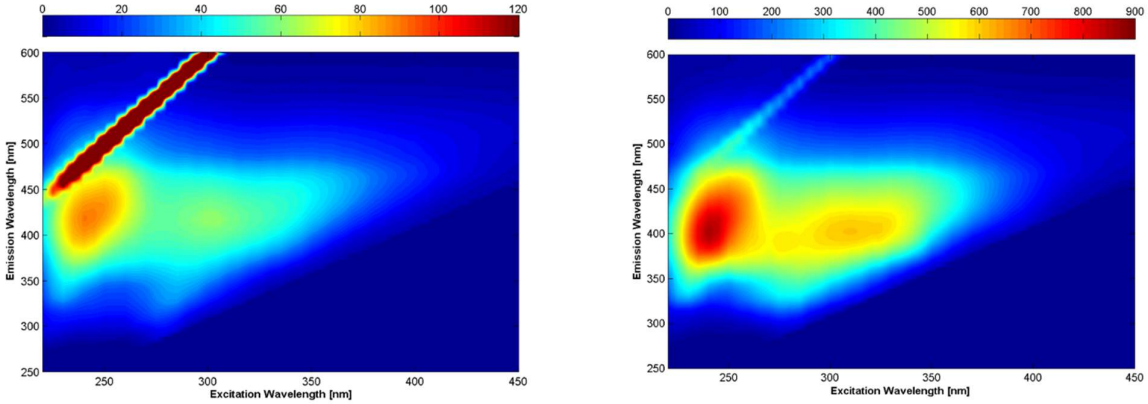

Figure A3. EEM fluorescence spectra of the aerosol WSOM samples collected in different time periods: day (left, 15/11/16) and night (right, 15/11/16 to 16/11/16)

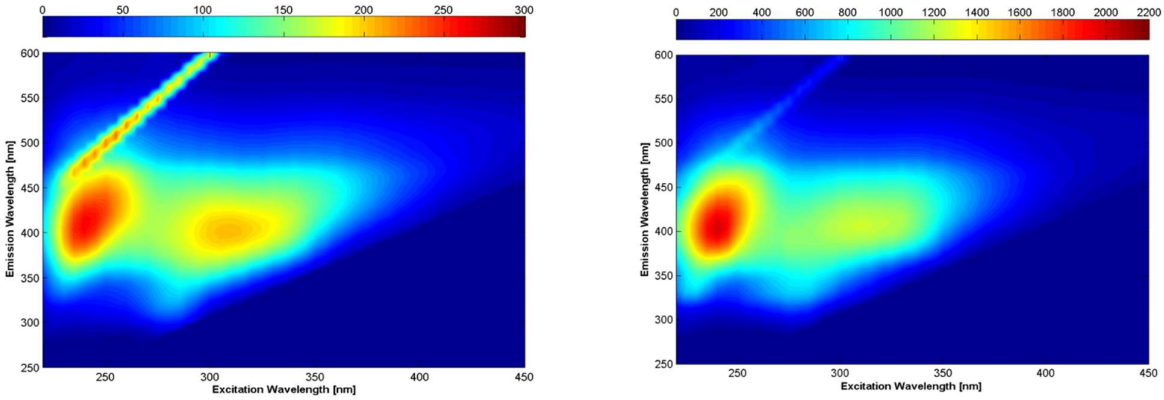

Figure A4. EEM fluorescence spectra of the aerosol WSOM samples collected in different time periods: day (left, 16/11/16) and night (right, 16/11/16 to 17/11/16)

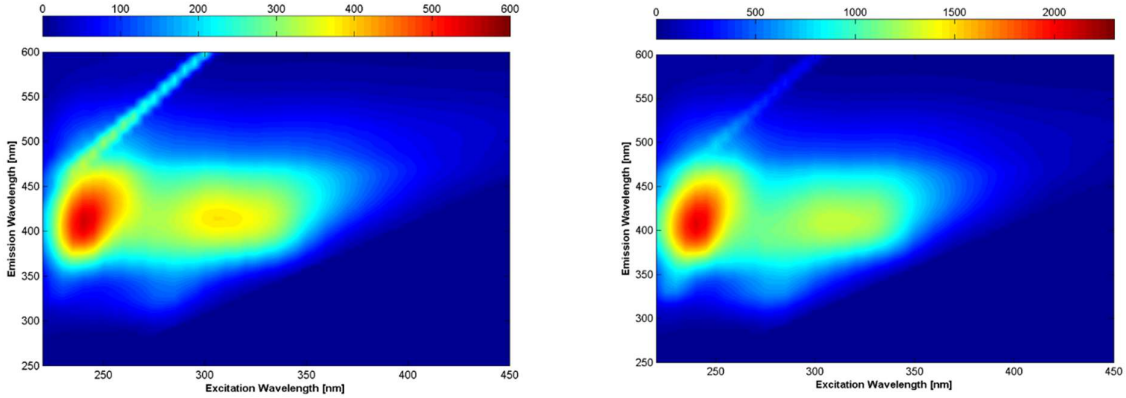

Figure A5. EEM fluorescence spectra of the aerosol WSOM samples collected in different time periods: day (left, 17/11/16) and night (right, 17/11/16 to 18/11/16)

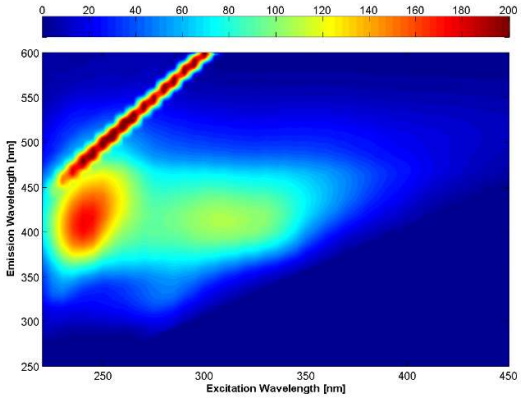

Figure A6. EEM fluorescence spectra of the aerosol WSOM sample collected during the day period (18/11/16)

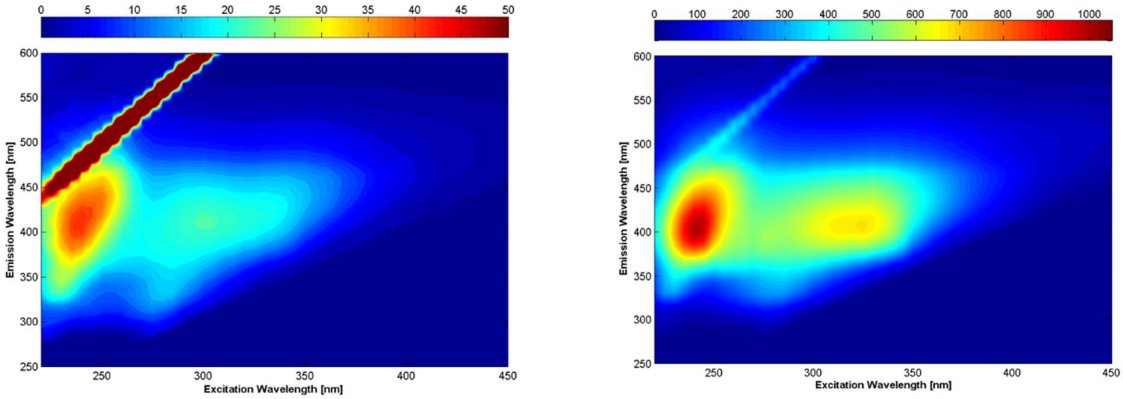

Figure A7. EEM fluorescence spectra of the aerosol WSOM samples collected in different time periods: day (left, 21/11/16) and night (right, 21/11/16 to 22/11/16)

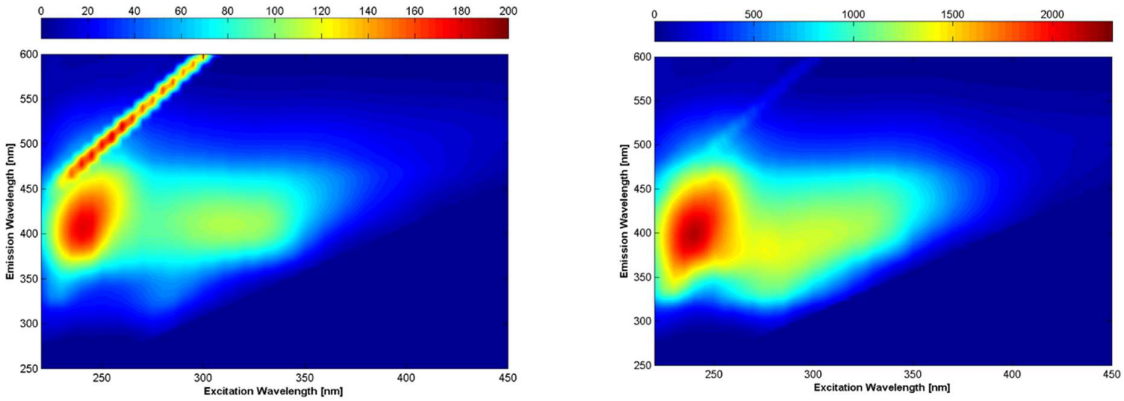

Figure A8. EEM fluorescence spectra of the aerosol WSOM samples collected in different time periods: day (left, 22/11/16) and night (right, 22/11/16 to 23/11/16)

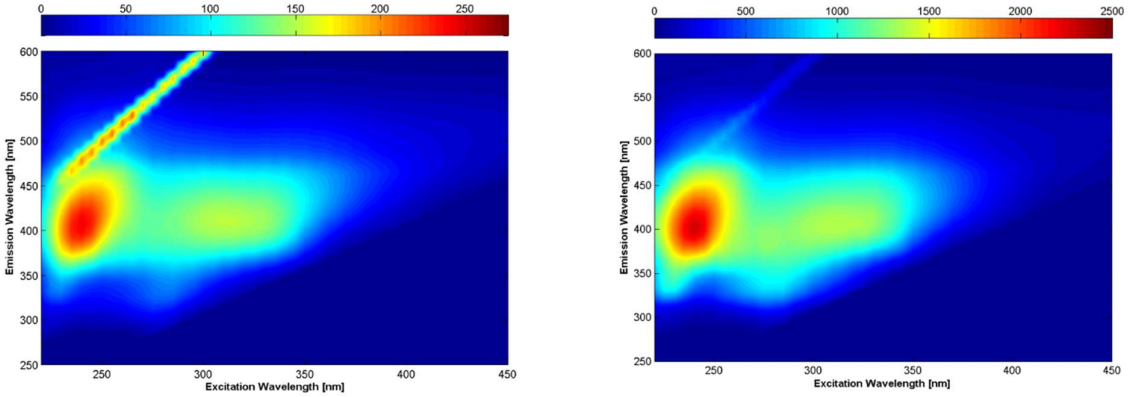

Figure A9. EEM fluorescence spectra of the aerosol WSOM samples collected in different time periods: day (left, 28/11/16) and night (right, 28/11/16 to 29/11/16)

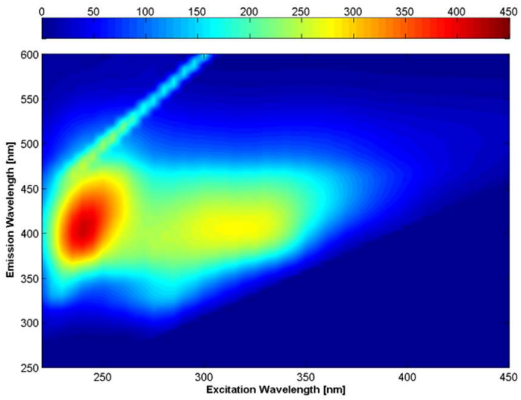

Figure A10. EEM fluorescence spectra of the aerosol WSOM sample collected during the day period (29/11/16)

A4. 2D NMR spectroscopy of fine urban aerosol WSOM samples

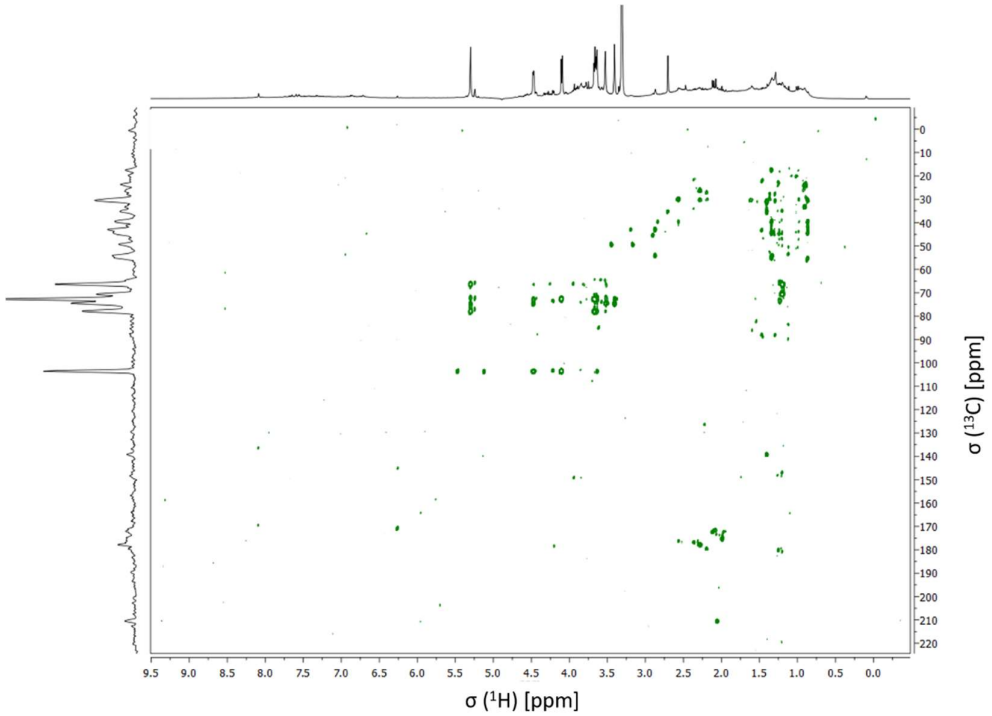

Figure A11. ^{1}H-^{13}C HMBC spectrum of the aerosol WSOM sample collected during day time periods

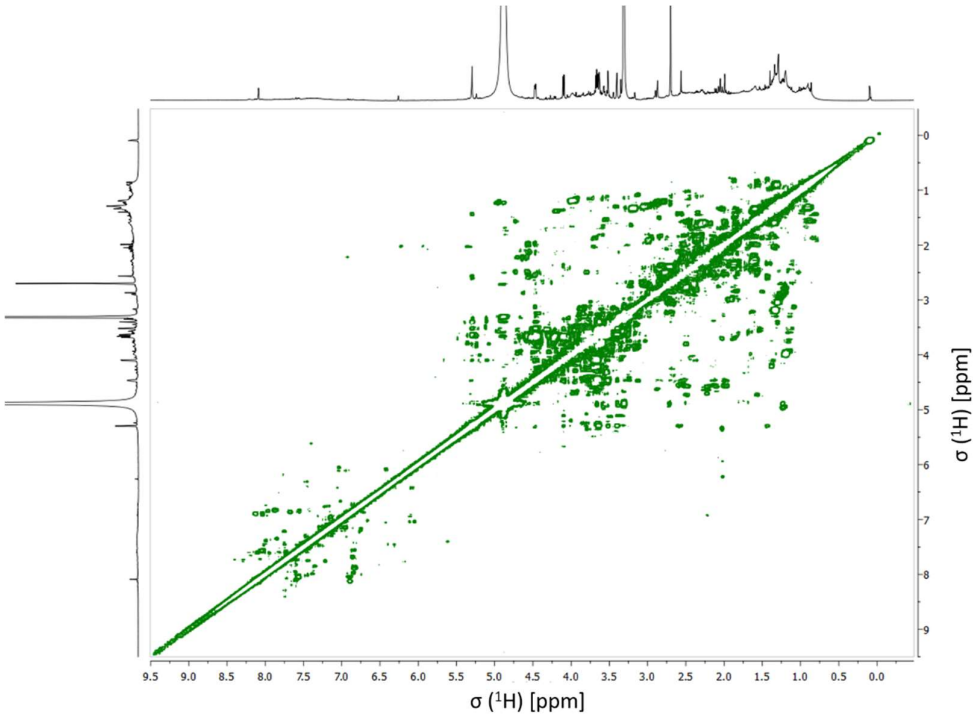

Figure A12. ^{1}H-^{1}H COSY spectrum of the aerosol WSOM sample collected during day time periods

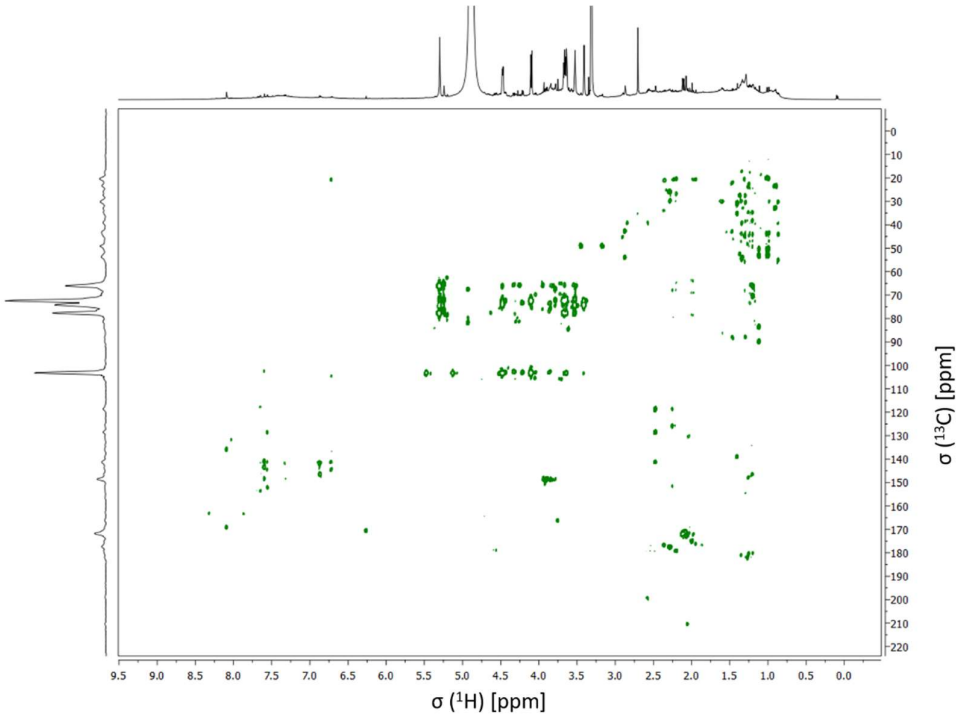

Figure A13. ^{1}H-^{13}C HMBC spectrum of the aerosol WSOM sample collected during night time periods

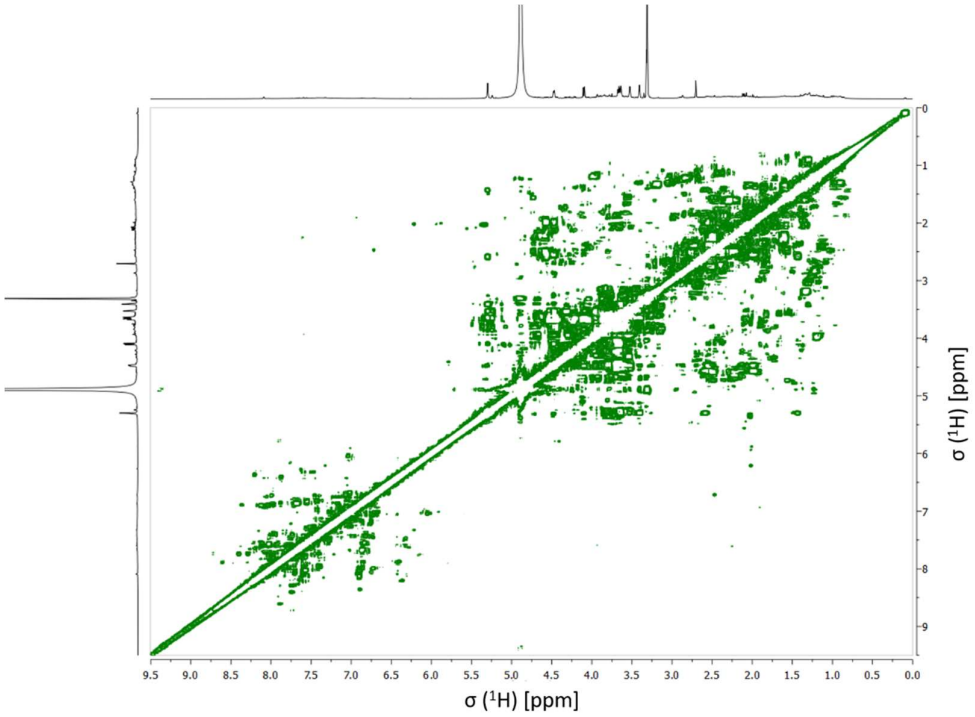

Figure A14. ^{1}H-^{1}H COSY spectrum of the aerosol WSOM sample collected during night time periods